Combinatorial, additive and dose-dependent drug–microbiome associations

Sofia Forslund, Rima Chakaroun, Maria Zimmermann-Kogadeeva, Lajos Markó, Judith Aron-Wisnewsky, Trine Nielsen, Lucas Moitinho-Silva, Thomas Schmidt, Gwen Falony, Sara Vieira-Silva, et al.

Combinatorial, additive and dose-dependent drug–microbiome associations

Sofia Forslund, Rima Chakaroun, Maria Zimmermann-Kogadeeva, Lajos Markó, Judith Aron-Wisnewsky, Trine Nielsen, Lucas Moitinho-Silva, Thomas Schmidt, Gwen Falony, Sara Vieira-Silva, et al.

Article

Combinatorial, additive and dose-dependent drug–microbiome associations

https://doi.org/10.1038/s41586-021-04177-9

Received: 7 September 2019

Accepted: 22 October 2021

Published online: 8 December 2021

Check for updates

Sofia K. Forslund[1,2,3,4,5,6,43], Rima Chakaroun[7,43], Maria Zimmermann-Kogadeeva[1,43], Lajos Markó[2,4,5,43], Judith Aron-Wisnewsky[8,9,43], Trine Nielsen[10,43], Lucas Moitinho-Silva[1], Thomas S. B. Schmidt[1], Gwen Falony[11], Sara Vieira-Silva[11], Solia Adriouch[8], Renato J. Alves[1], Karen Assmann[8], Jean-Philippe Bastard[12,13], Till Birkner[2,3], Robert Caesar[14], Julien Chilloux[15], Luis Pedro Coelho[1,16,17], Leopold Fezeu[18], Nathalie Galleron[19], Gerard Helft[20], Richard Isnard[20], Boyang Ji[21], Michael Kuhn[1], Emmanuelle Le Chatelier[19], Antonis Myridakis[15], Lisa Olsson[14], Nicolas Pons[19], Edi Prifti[8,22,23], Benoit Quinquis[19], Hugo Roume[19], Joe-Elie Salem[24], Nataliya Sokolovska[8], Valentina Tremaroli[14], Mireia Valles-Colomer[11], Christian Lewinter[25], Nadja B. Søndertoft[10], Helle Krogh Pedersen[10], Tue H. Hansen[10], The MetaCardis Consortium*, Jens Peter Gøtze[26], Lars Køber[25], Henrik Vestergaard[10,27], Torben Hansen[10], Jean-Daniel Zucker[8,22,23], Serge Hercberg[18], Jean-Michel Oppert[9], Ivica Letunic[1,28], Jens Nielsen[21], Fredrik Bäckhed[10,14,29], S. Dusko Ehrlich[19], Marc-Emmanuel Dumas[15,30,31,32], Jeroen Raes[11], Oluf Pedersen[10], Karine Clément[8,9]✉, Michael Stumvoll[7,33]✉ & Peer Bork[1,3,34,35]✉

During the transition from a healthy state to cardiometabolic disease, patients become heavily medicated, which leads to an increasingly aberrant gut microbiome and serum metabolome, and complicates biomarker discovery[1–5]. Here, through integrated multi-omics analyses of 2,173 European residents from the MetaCardis cohort, we show that the explanatory power of drugs for the variability in both host and gut microbiome features exceeds that of disease. We quantify inferred effects of single medications, their combinations as well as additive effects, and show that the latter shift the metabolome and microbiome towards a healthier state, exemplified in synergistic reduction in serum atherogenic lipoproteins by statins combined with aspirin, or enrichment of intestinal *Roseburia* by diuretic agents combined with beta-blockers. Several antibiotics exhibit a quantitative relationship between the number of courses prescribed and progression towards a microbiome state that is associated with the severity of cardiometabolic disease. We also report a relationship between cardiometabolic drug dosage, improvement in clinical markers and microbiome composition, supporting direct drug effects. Taken together, our computational framework and resulting resources enable the disentanglement of the effects of drugs and disease on host and microbiome features in multimedicated individuals. Furthermore, the robust signatures identified using our framework provide new hypotheses for drug–host–microbiome interactions in cardiometabolic disease.

Identifying robust contributions of gut microbiota to health and disease requires complex technical and statistical frameworks[1,2] and remains challenging due to the many covariates that affect both microbial composition[3–5] and disease. Common covariates include therapeutic drugs[4,6–10]—such as broadly prescribed proton-pump inhibitors (PPIs)[6] and the type 2 diabetes (T2D) drug metformin[7]—that affect the gut microbiota and modulate inflammation[11]. Furthermore, direct drug–microbial interactions have been demonstrated in vitro[8]. For several drugs in a mostly healthy population, their usage explained more variance in microbiota composition than other covariates tested, albeit with small individual effect sizes[12]. However, studies in healthy populations[12,13] are inadequate for investigating the secondary effects of drugs in the context of chronic diseases. To robustly disentangle drug–microbiome associations from host and disease factors, large sample sizes and a high resolution of clinical phenotypes and medication are required, while accounting for variables known to affect the gut microbiome. Finally, drug effects are often dose-dependent, yet dosage is rarely considered in microbiome studies.

To overcome these limitations, we propose a general framework for separating disease from treatment associations in multi-omics cross-sectional studies and apply it to gut metagenomic, host clinical and metabolomic measurements of 2,173 European residents from the multicentre MetaCardis cohort. The MetaCardis cohort includes patients with metabolic syndrome, severe and morbid obesity, T2D, acute and chronic coronary artery disease and heart failure, and healthy control individuals. Considering cardiometabolic disease (CMD) and herein frequently prescribed medications, we investigated drug–host–microbiome associations for eight major indications (antidiabetic,

A list of affiliations appears at the end of the paper.

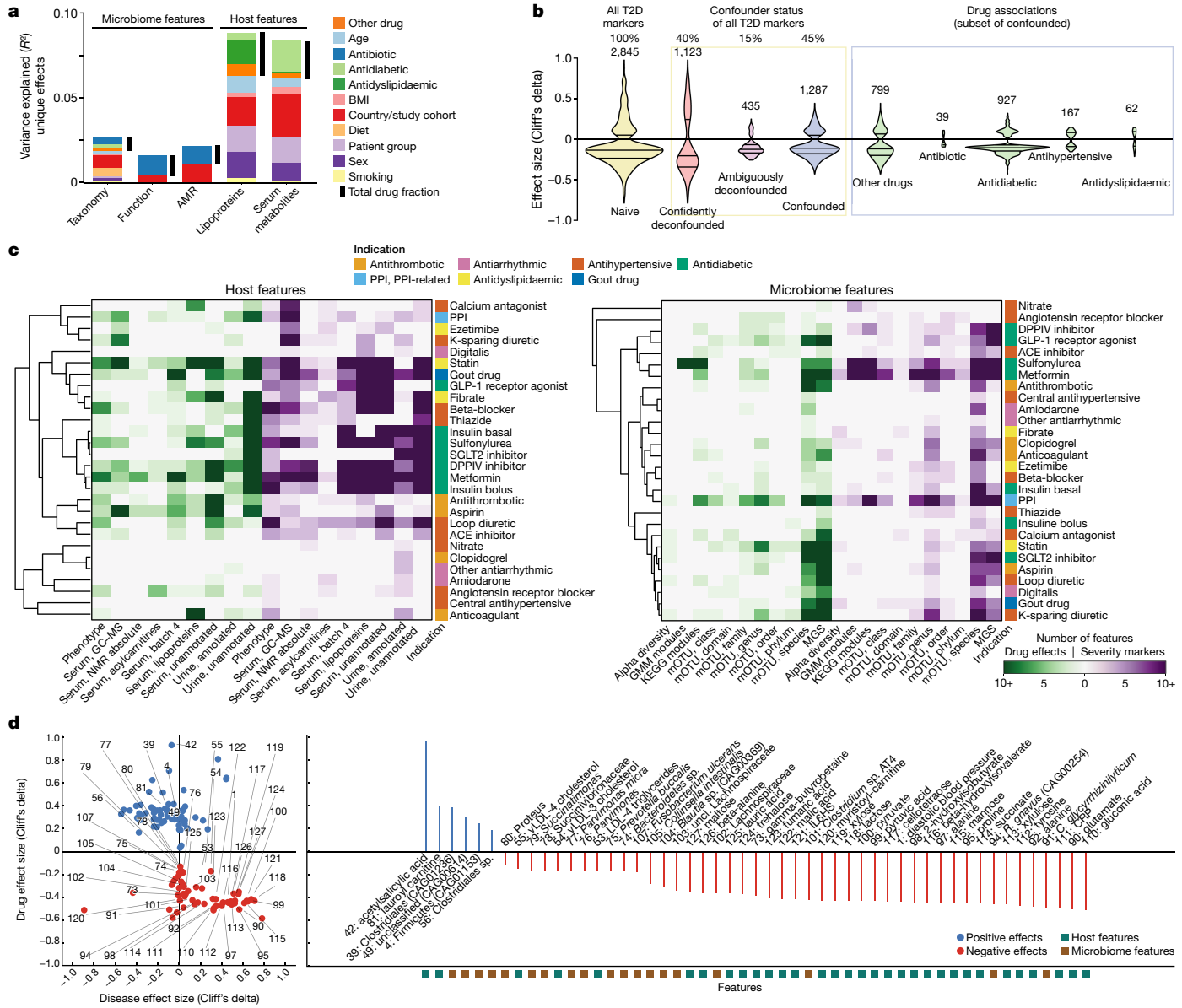

Fig. 1 | Associations between CMD drugs, host and microbiome. a, The variance explained (R^2) by variable group and feature type. **b**, Confounder analysis of features that are differentially abundant between individuals with T2D and control individuals. Data are the distribution of effect size; the number of features per category is listed. Naive associations (yellow, two-sided MWU, FDR < 0.1) are either confounded or ambiguously/confidently deconfounded (blue, purple and red violins). The green violins show the breakdown of confounders by drug category. **c**, Hierarchical clustering of host (left) and microbiome (right) features associated with each drug in at least one patient group. Features separate into potential drug effects (discordant with disease associations) and severity markers (concordant with disease associations). GC–MS, gas chromatography coupled with mass spectrometry; MGS, metagenomic species; mOTU, metagenomic operational taxonomic units; NMR, nuclear magnetic resonance. **d**, Effect sizes (Cliff's delta) of confidently deconfounded associations between aspirin usage and features versus disease effect size within each clinical group (left). Right, a subset of features is highlighted for interpretation. Uncl., unclassified.

antihypertensive, antidyslipidaemic, antithrombotic, antiarrhythmic agents, gout medication, PPIs and antibiotics). The most commonly prescribed CMD drugs were statins (n = 772, 35.5%), beta-blockers (n = 656, 30.2%), metformin (n = 607, 27.9%), aspirin (n = 532, 24.5%), angiotensin converting enzyme (ACE) inhibitors (n = 470, 21.6%) and angiotensin II receptor blockers (n = 470, 21.6%), often taken in combination (Supplementary Tables 1–4). We therefore studied individual drug effects, and their synergistic and additive interactions in the context of available phenotypic, dietary and demographic variables, molecular readouts including serum concentrations of lipoproteins, cytokines and metabolites, and taxonomic and functional profiles of the gut microbiome.

To quantify the overall effect of medications, we performed multivariate regression analysis of the explained variance in host and microbiome data on the total influence of medications, clinical and environmental factors and disease status. All of the drugs together explain more variation in microbiome composition than disease group alone, or any other factor considered under a conservative estimate. However, consistent with previously reported high individual variability[14], only 1.7–9% of variation between individuals is explainable by factors that are included in the model, of which 1–2.5% is attributable to drug intake, comparable to disease status, diet and smoking combined (Fig. 1a and Supplementary Table 5).

To quantify individual drug effects, we implemented a univariate statistical approach to disentangle drugs from disease associations with the gut microbiome and host features. Thus, features distinguishing patient groups from healthy controls are divided into (1) confidently

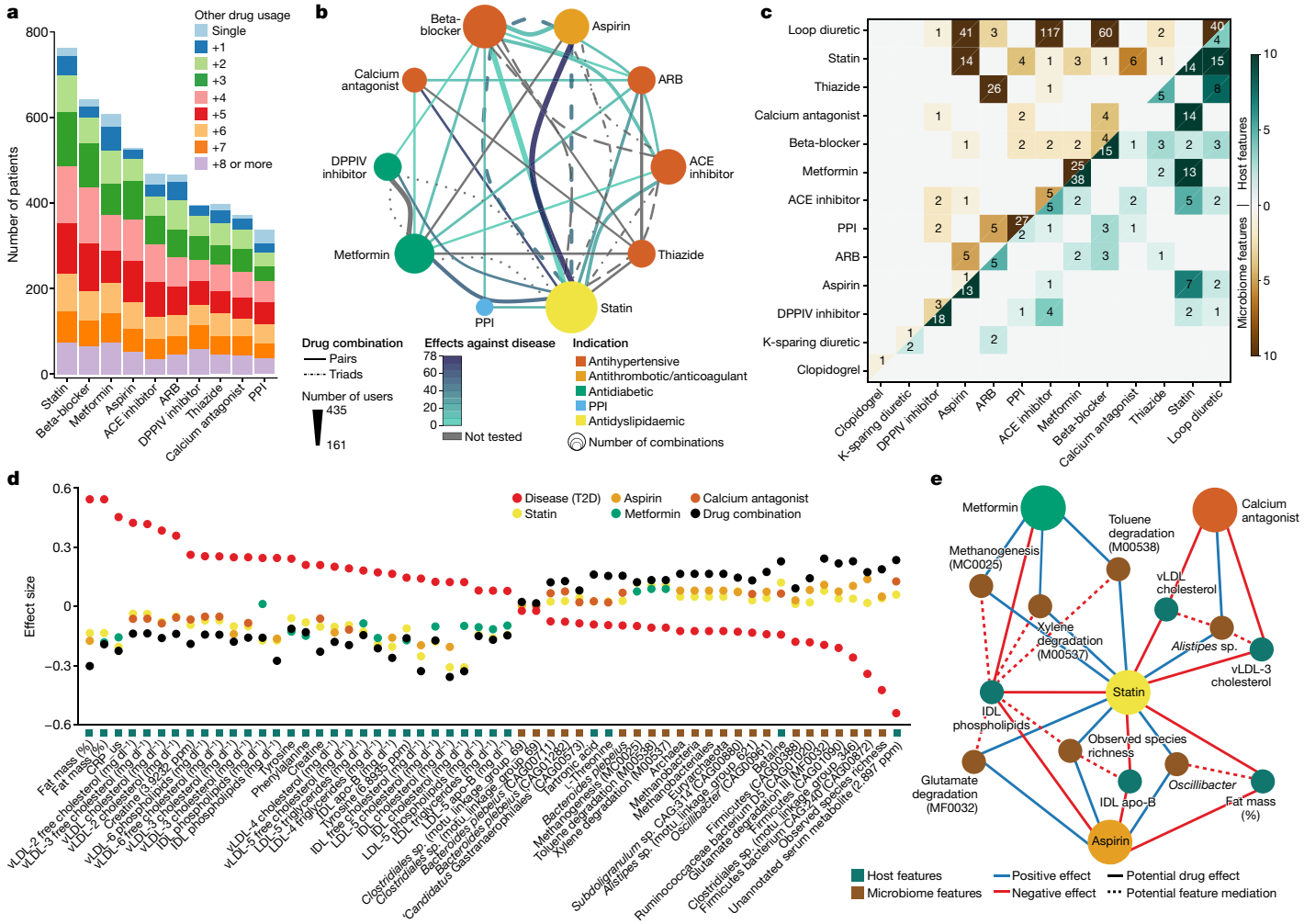

Fig. 2 | Combinatorial effects of CMD drugs. a, The number of patients with CMD receiving each drug in combination with a specified number of other drugs. **b**, The 30 most common drug combinations. The node size is proportional to the number of combinations. The edge width is proportional to the number of users per combination. The line colour corresponds to the number of significant drug associations. The solid lines indicate drug pairs; the dotted/dashed lines indicate drug triplets. **c**, The number of features (host (bottom, green) and microbiome (top, brown)) that are affected by each drug combination more strongly than by single drugs among patients with T2D. The diagonal values show the number of features that are affected by each drug alone. **d**, The effect size (Cliff's delta) of disease associations (red), drug combinations (black) and single drugs (other colours) among patients with T2D for the combination of statin with metformin, aspirin or calcium antagonist. Each item on the *x* axis corresponds to a drug-combination–feature association. IDL, intermediate-density lipoprotein. **e**, Drug–feature graph showing the potential mediation between host and microbiome features. The colour of the solid lines represents the direction of drug effect. The colour of the dashed lines represents the sign of Pearson's correlation coefficient ($P < 0.1$) between potentially mediated features (Supplementary Tables 8–10).

deconfounded features of CMD; (2) ambiguously deconfounded (where both treatment and disease strongly correlate); and (3) confounded (unambiguous drug associations) (Extended Data Fig. 1). A major fraction of naive associations (for example, 45% for T2D) between drugs and microbiome or metabolome is attributable to drug intake (Fig. 1b and Supplementary Table 5). Nonetheless, we recovered previously described signatures of metabolic disease and show that these cannot be reduced to treatment effects (Extended Data Fig. 2 and Supplementary Results). We therefore conclude that a drug-conscious approach uncovers true disease associations and is crucial to circumvent highly inflated treatment-confounded false-positives in biomarker discovery.

Next, we disentangled the potential direct effects of medication (for which the treatment association direction opposes the disease association) from potential severity markers (concordant direction of the treatment and disease association). Of 28 cardiometabolic drugs taken by at least ten individuals within at least one patient group, the strongest effects on the serum metabolome were found for antidiabetic drugs, statins, beta-blockers, antithrombotic drugs and aspirin. Although drugs with the same indication (that is, antidiabetic, antihypertensive) had concordant associations with host features, the effect on the gut microbiome was more diverse in the effect size and the direction between these drugs (Fig. 1c and Supplementary Tables 6 and 7). Our approach recaptured previously reported findings on the effect of antibiotics[15], PPIs[16,17], statins[11], beta-blockers and metformin[7,18] (Extended Data Fig. 3). Importantly, we identified new associations for these as well as for other highly prevalent drugs (Supplementary Results). For example, we identified aspirin-associated changes in the abundances of microbial species, and shifts in the serum lipidome and metabolome associated with improved cardiometabolic health (among others, depletion of *Ruminococcus gnavus*, *Clostridium glycyrrhizinilyticum* and *Parvimonas micra*, reduction in the plasma concentrations of inflammatory markers (CRP and IL-6), and decreased levels of pyruvate, glutamate and succinate at comparable significance to that of the aspirin levels detected in the serum of medicated individuals; Fig. 1d). Moreover, γ-butyrobetaine, which is a recently identified proatherogenic intermediate of microbial metabolism[19], is lower in individuals taking aspirin, revealing a

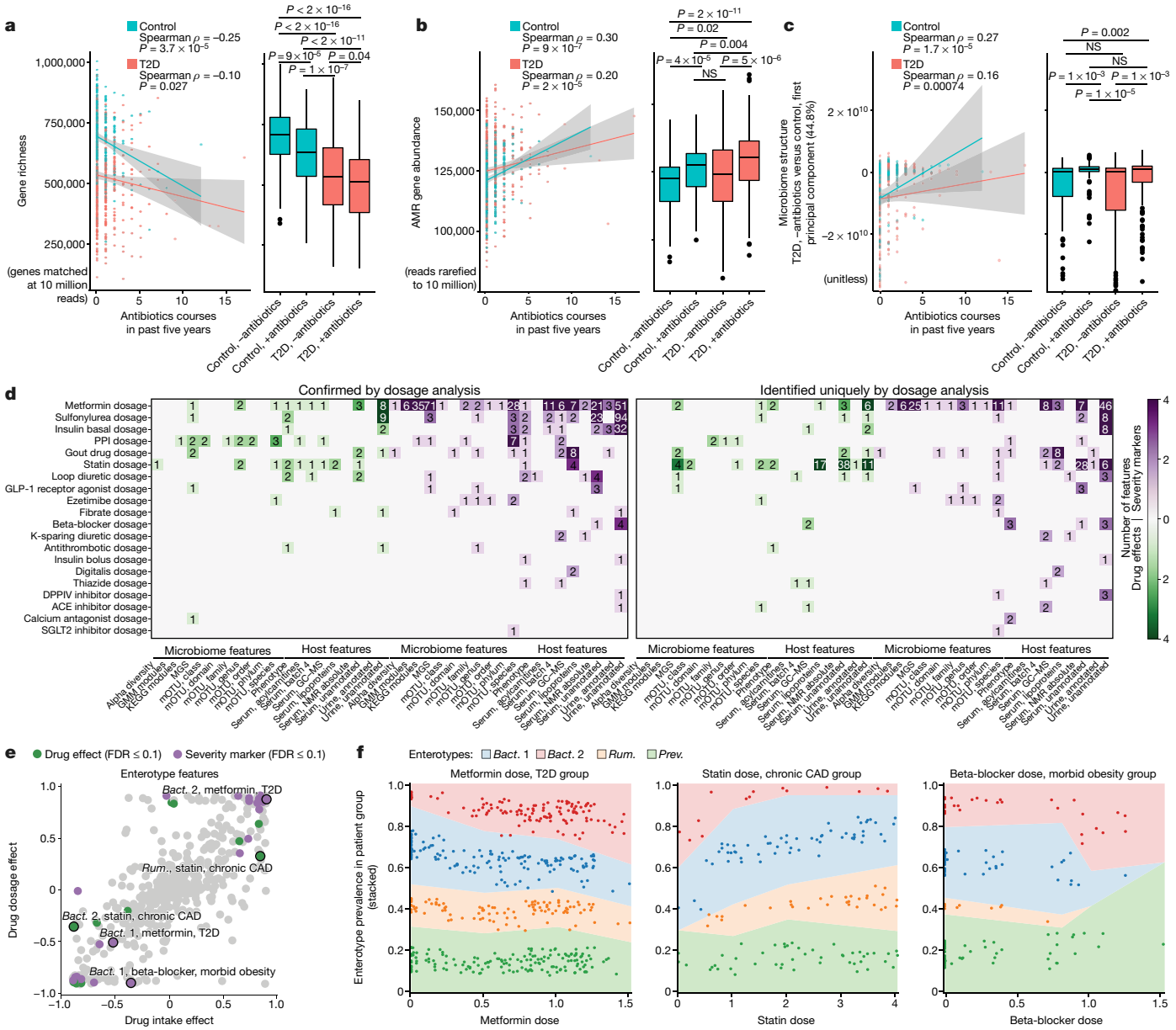

Fig. 3 | Additive and dose-dependent drug associations with the host and microbiome. a–**c**, Microbiome features that are significantly associated with the number of antibiotics courses in the past 5 years in control individuals ($n = 256$) and individuals with T2D ($n = 456$). **a**, Gene richness. **b**, The total abundance of antimicrobial resistance genes. **c**, The first principal component of gut species composition. For **a**–**c**, the grey area shows the 95% confidence intervals for the linear regression. The box plots (median (centre line), quartiles (box limits), 1.5× interquartile range (whiskers) and outliers (dots)) show the comparisons in antibiotics-naive ($n = 148$ (control), $n = 274$ (T2D)) and antibiotics-exposed ($n = 108$ (control), $n = 182$ (T2D)) control individuals and individuals with T2D. Pairwise significance values (two-sided MWU tests, FDR-adjusted) are shown in the figure. **d**, The number of drug–feature associations confirmed by dosage analysis (left), or uniquely revealed by dosage analysis (right). Features are separated by potential drug effects (discordant with the disease effect) or severity markers (concordant with the disease effect). **e**, The relationship between drug intake effect size (Cliff's delta) and drug dosage effect size (Spearman's ρ) on enterotype distribution within each patient group. Features that are significantly affected in either analysis (two-sided MWU, FDR < 0.1) are shown in green (potential drug effects) or purple (potential severity markers). The black circles highlight associations that are depicted in **f**. *Bact.*, *Bacteroides*; *Prev.*, *Prevotella*; *Rum.*, *Ruminococcus*. **f**, The coloured areas represent the stacked enterotype prevalence along the drug dosage axis. Each dot represents a patient taking a specific drug dose, and is classified into one of the four enterotypes. Random noise was added for better visualization (Supplementary Tables 11–14).

potential complex antiatherogenic effect of the drug beyond its known platelet-inhibitory functions[20]. For metformin, we deduced new anti-diabetic effects that are possibly related to lowered glutamate levels[21] ($d = -0.17$, false-discovery rate (FDR)-adjusted $P = 0.02$), due to reduced microbial glutamate transport ($d = -0.2$, FDR-adjusted $P = 0.006$), along with increased microbial vitamin B12 uptake ($d = 0.32$, FDR-adjusted $P = 3.65 \times 10^{-6}$), potentially contributing to vitamin B12 deficiency in the host—a known side effect of metformin (Supplementary Results and Supplementary Table 6). PPIs had the most associations with the gut microbiome features (Fig. 1c and Supplementary Table 7), including a higher prevalence of presumably oral bacteria, supporting the hypothesized PPI-caused transfer of oral bacteria into the gut due to decreased stomach acidity[17]. Single-nucleotide variation analysis on the basis of large reference cohorts revealed an increased abundance of oral-based strains of *Rothia*, *Haemophilus* and *Streptococcus* species in the gut of individuals taking PPIs, implying that the patient's own oral

strains colonize the intestine as gastric acidity weakens[22] (Extended Data Fig. 4 and Supplementary Results).

Beyond single drugs, MetaCardis enables the analysis of combinatorial (polypharmacy) effects, as 1,300 individuals were prescribed more than one drug (average intake of 3 drugs with some receiving up to 13 distinct drugs per day) (Fig. 2a, b and Supplementary Tables 2 and 3). Polypharmacy in CMD mostly reflects the concurrence of metabolic diseases, risk factors or treatments preventing the recurrence of an atherosclerotic event, but also includes medications that are co-prescribed to reduce side effects, such as PPIs with aspirin to prevent gastric ulcers and bleeding. Multimedicated patients often exhibit a more pronounced improvement in disease markers compared with those receiving only one of the drugs, consistent with synergistic interactions between drugs. In the T2D group, the most pronounced synergistic effects on the microbiome features were observed for loop diuretics, especially in combination with aspirin, ACE inhibitors and beta-blockers, whereas the most pronounced synergistic effects on host features were observed for statins (Fig. 2c). For example, loop diuretics combined with aspirin, ACE inhibitors or beta-blockers more strongly enrich microbiome-related health markers[23], including *Roseburia* abundance[11] (combination: $d = 0.46$, $d = 0.51$, $d = 0.36$, respectively; single drugs: diuretics $d = 0.27$). Taken with metformin or aspirin, statins are associated with lower intermediate-density, low-density (LDL) and very-low-density (vLDL) lipoprotein levels in the serum, and lower total body fat mass, while increasing the microbiome richness and abundance of Firmicutes and methanogenic bacteria that are depleted in the T2D group (Fig. 2d and Supplementary Tables 8 and 9). These shifts in the microbiome might mediate some of the synergistic drug effects on the host (Fig. 2e, Supplementary Table 10 and Supplementary Results).

Next, we investigated additive drug associations. The clearest such association was observed for antibiotics using five-year retrospective exposure (total number of courses). Antibiotics are frequently prescribed for patients with CMD due to an increased prevalence of infections[24]. Yet, epidemiological studies link antibiotics to an increased risk of obesity, T2D, and metabolic and inflammatory diseases[25]. Previous antibiotics exposure is significantly associated with lower gut gene richness within the same participant groups (Fig. 3a; Spearman $\rho = -0.25$, $P = 3.7 \times 10^{-5}$) and correlated with the total abundance of antimicrobial resistance genes in the gut (control individuals: Spearman $\rho = 0.30$, $P = 9 \times 10^{-7}$; individuals with T2D: Spearman $\rho = 0.20$, $P = 2 \times 10^{-5}$) (Fig. 3b). These findings imply that there are cumulative, additive shifts after repeated antibiotics exposure towards a more resistant but less diverse microbiota, which is a hallmark of the microbiome signature in obesity, insulin resistance and low-grade inflammation[26]. The same properties distinguish antibiotics-naive patients with CMD from healthy control individuals, confirming an effect of repeated antibiotics exposure (antibiotics-naive healthy versus T2D richness, two-sided Mann–Whitney U (MWU)-test, $P = 7.9 \times 10^{-21}$; antimicrobial resistance gene abundance, $P = 2 \times 10^{-2}$). Using principal component analysis (Supplementary Table 11), we show that the first principal component of microbiome composition, which explains 45% of variation and correlates with gene richness, is associated with both an additive effect of antibiotics and metabolic impairment after antibiotics exposure (antibiotics effect: controls, Spearman $\rho = 0.27$, $P = 1.7 \times 10^{-5}$; individuals with T2D, Spearman $\rho = 0.16$, $P = 7 \times 10^{-4}$; antibiotics-naive healthy individuals versus antibiotics-treated healthy individuals, two-sided MWU test, $P = 1 \times 10^{-3}$; antibiotics-naive individuals with T2D versus antibiotics-treated individuals with T2D, two-sided MWU test, $P = 1 \times 10^{-3}$) (Fig. 3c). A multivariate breakdown of these shifts reveals a reduced abundance of *Prevotella copri* and *Faecalibacterium prausnitzii*, and an increase in *Bacteroides vulgatus* and *Bacteroides dorei*, representatives of abundant genera constituting hallmarks of enterotypes[27,28]. Furthermore, we show that shifts in gut microbial metabolic functions link additive effects of specific antibiotics groups to CMD susceptibility (Extended Data Figs. 5–7, Supplementary Table 12 and Supplementary Results).

Moreover, the detailed medication tracking in MetaCardis enables us to investigate the effect of dosage on the host and microbiota. For the 20 drugs with sufficient dosage information, we distinguished between dosage-confirmed effects, that is, features that are significantly associated with both drug intake and its dosage; and dosage-unique effects, where dosage analysis revealed associations that are not captured by other analyses. The drugs with the most features confirmed by dosage analysis were metformin, sulfonylurea, insulin, PPI, gout medications and statins, whereas the most dosage-unique associations were reported for metformin and statins (Fig. 3d). Statin dosage was negatively associated with atherogenic vLDL levels, highlighting the intended dose-dependent lipid-lowering effects, and positively associated with health-promoting *Roseburia* species in the gut[11]. Metformin dosage was negatively associated with cytokine levels (SDF1 and MIF), consistent with previous reports of its anti-inflammatory effects[29,30]. Furthermore, we observed a change in the prevalence of the *Bacteroides* 1 and *Bacteroides* 2 enterotypes in patients with increasing metformin dosage; the *Bacteroides* 2 enterotype is also associated with disease, proposing it as a severity marker in T2D indepedent of metformin treatment (Fig. 3e, f and Supplementary Tables 13 and 14). For statins, dosage analysis strengthens the reported observation of microbiome shifts towards a heathier state away from the *Bacteroides* 2 enterotype[11]. Moreover, dosage analysis uniquely identified *Bacteroides* 2 and *Prevotella* enterotypes as severity markers for beta-blocker usage in individuals with severe and morbid obesity (Fig. 3e, f and Supplementary Table 14).

With stringent analytical approaches, we show that not only medication intake, but also dosage, drug combinations and previous exposure to antibiotics should be captured in human studies to disentangle the drug–host–microbiome interactions in complex diseases. For several drugs, our results identify microbiome shifts associated with medication intake that might mediate the improvement in clinical markers. Given the observational study design, our analysis enables the identification of associative (and not necessarily causative) effects of drugs on variations in the microbiome and clinical phenotypes. Thus, experimental validation in animal models (such as the multimodal effect of low-dose aspirin, or the synergistic effects of statin and aspirin or metformin in LDL-receptor-deficient mice fed a high-fat diet) is required to substantiate these findings, as controlled clinical trials can be challenging in a population with multimorbidity. Disentangling medication effects on the gut microbiome and serum metabolome, as illustrated here, is the first step towards understanding the systemic effects of drugs at the molecular level, while preclinical tests should be performed to assess their significance in terms of health outcomes for CMD. To improve treatment in the context of genetic and microbiome variability and complex drug regimens, robust molecular markers are needed to identify the transition from a state of good health to chronic disease. Subsequently, the gut modulation potential of drugs could be harnessed to reverse disease progression in a personalized manner.

Online content

Any methods, additional references, Nature Research reporting summaries, source data, extended data, supplementary information, acknowledgements, peer review information; details of author contributions and competing interests; and statements of data and code availability are available at https://doi.org/10.1038/s41586-021-04177-9.

1. Sinha, R. et al. Assessment of variation in microbial community amplicon sequencing by the Microbiome Quality Control (MBQC) project consortium. *Nat. Biotechnol.* **35**, 1077–1086 (2017).
2. Costea, P. I. et al. Towards standards for human fecal sample processing in metagenomic studies. *Nat. Biotechnol.* **35**, 1069–1076 (2017).
3. Rothschild, D. et al. Environment dominates over host genetics in shaping human gut microbiota. *Nature* **555**, 210–215 (2018).

4. Schmidt, T. S. B., Raes, J. & Bork, P. The human gut microbiome: from association to modulation. *Cell* **172**, 1198–1215 (2018).
5. Vujkovic-Cvijin, I. et al. Host variables confound gut microbiota studies of human disease. *Nature* **587**, 448–454 (2020).
6. Tsuda, A. et al. Influence of proton-pump inhibitors on the luminal microbiota in the gastrointestinal tract. *Clin. Transl. Gastroenterol.* **6**, e89 (2015).
7. Forslund, K. et al. Disentangling type 2 diabetes and metformin treatment signatures in the human gut microbiota. *Nature* **528**, 262–266 (2015).
8. Maier, L. et al. Extensive impact of non-antibiotic drugs on human gut bacteria. *Nature* **555**, 623–628 (2018).
9. Le Bastard, Q. et al. Systematic review: human gut dysbiosis induced by non-antibiotic prescription medications. *Aliment. Pharmacol. Ther.* **47**, 332–345 (2018).
10. Vich Vila, A. et al. Impact of commonly used drugs on the composition and metabolic function of the gut microbiota. *Nat. Commun.* **11**, 362 (2020).
11. Vieira-Silva, S. et al. Statin therapy is associated with lower prevalence of gut microbiota dysbiosis. *Nature* **581**, 310–315 (2020).
12. Falony, G. et al. Population-level analysis of gut microbiome variation. *Science* **352**, 560–564 (2016).
13. Jackson, M. A. et al. Gut microbiota associations with common diseases and prescription medications in a population-based cohort. *Nat. Commun.* **9**, 2655 (2018).
14. Conlon, M. A. & Bird, A. R. The impact of diet and lifestyle on gut microbiota and human health. *Nutrients* **7**, 17–44 (2014).
15. Blaser, M. J. Antibiotic use and its consequences for the normal microbiome. *Science* **352**, 544–545 (2016).
16. Imhann, F. et al. Proton pump inhibitors affect the gut microbiome. *Gut* **65**, 740–748 (2016).
17. Imhann, F. et al. The influence of proton pump inhibitors and other commonly used medication on the gut microbiota. *Gut Microbes* **8**, 351–358 (2017).
18. Wu, H. et al. Metformin alters the gut microbiome of individuals with treatment-naive type 2 diabetes, contributing to the therapeutic effects of the drug. *Nat. Med.* **23**, 850–858 (2017).
19. Koeth, R. A. et al. γ-Butyrobetaine is a proatherogenic intermediate in gut microbial metabolism of L-carnitine to TMAO. *Cell Metab.* **20**, 799–812 (2014).
20. Kopp, E. & Ghosh, S. Inhibition of NF-κB by sodium salicylate and aspirin. *Science* **265**, 956–959 (1994).
21. Davalli, A. M., Perego, C. & Folli, F. B. The potential role of glutamate in the current diabetes epidemic. *Acta Diabetol.* **49**, 167–183 (2012).
22. Schmidt, T. S. et al. Extensive transmission of microbes along the gastrointestinal tract. *eLife* **8**, e42693 (2019).
23. Shimazu, T. et al. Suppression of oxidative stress by β-hydroxybutyrate, an endogenous histone deacetylase inhibitor. *Science* **339**, 211–214 (2012).
24. Shah, B. R. & Hux, J. E. Quantifying the risk of infectious diseases for people with diabetes. *Diabetes Care* **26**, 510–513 (2003).
25. Korpela, K. & Vos, W. M. de. Antibiotic use in childhood alters the gut microbiota and predisposes to overweight. *Microbial Cell* **3**, 296–298 (2016).
26. Le Chatelier, E. et al. Richness of human gut microbiome correlates with metabolic markers. *Nature* **500**, 541–546 (2013).
27. Arumugam, M. et al. Enterotypes of the human gut microbiome. *Nature* **473**, 174–180 (2011).
28. Costea, P. I. et al. Enterotypes in the landscape of gut microbial community composition. *Nat. Microbiol.* **3**, 8–16 (2018).
29. Cameron, A. R. et al. Anti-inflammatory effects of metformin irrespective of diabetes status. *Circ. Res.* **119**, 652–665 (2016).
30. Dandona, P. et al. Increased plasma concentration of macrophage migration inhibitory factor (MIF) and MIF mRNA in mononuclear cells in the obese and the suppressive action of metformin. *J. Clin. Endocrinol. Metab.* **89**, 5043–5047 (2004).

[1]Structural and Computational Biology Unit, European Molecular Biology Laboratory, Heidelberg, Germany. [2]Max Delbrück Center for Molecular Medicine (MDC), Berlin, Germany. [3]Charité–Universitätsmedizin Berlin, Berlin, Germany. [4]Experimental and Clinical Research Center, A Cooperation of Charité–Universitätsmedizin and the Max-Delbrück Center, Berlin, Germany. [5]Berlin Institute of Health (BIH), Berlin, Germany. [6]DZHK (German Centre for Cardiovascular Research), Partner Site Berlin, Berlin, Germany. [7]Medical Department III—Endocrinology, Nephrology, Rheumatology, University of Leipzig Medical Center, Leipzig, Germany. [8]Nutrition and Obesities; Systemic Approaches (NutriOmics), Sorbonne Université, INSERM, Paris, France. [9]Nutrition Department, Assistance Publique Hôpitaux de Paris, Pitie-Salpêtrière Hospital, Paris, France. [10]Novo Nordisk Foundation Center for Basic Metabolic Research, Faculty of Health and Medical Sciences, University of Copenhagen, Copenhagen, Denmark. [11]Center for Microbiology, VIB, and Rega Institute, KU Leuven, Leuven, Belgium. [12]Assistance Publique Hôpitaux de Paris, UF Biomarqueurs Inflammatoires et Métaboliques, Biochemistry and Hormonology Department, Tenon Hospital, Paris, France. [13]Centre de Recherche Saint-Antoine, Sorbonne Université, INSERM UMR S938, Paris, France. [14]Wallenberg Laboratory, Department of Molecular and Clinical Medicine, Sahlgrenska Center for Cardiovascular and Metabolic Research, University of Gothenburg, Gothenburg, Sweden. [15]Division of Systems Medicine, Department of Metabolism, Digestion and Reproduction, Faculty of Medicine, Imperial College London, London, UK. [16]Institute of Science and Technology for Brain-Inspired Intelligence, Fudan University, Shanghai, China. [17]MOE Key Laboratory of Computational Neuroscience and Brain-Inspired Intelligence, and MOE Frontiers Center for Brain Science, Shanghai, China. [18]Nutritional Epidemiology Research Team (EREN), Sorbonne Paris Cité Epidemiology and Statistics Research Centre (CRESS), U1153 INSERM, U1125, INRA, CNAM, University of Paris 13, Paris, France. [19]Metagenopolis, INRA, AgroParisTech, Université Paris-Saclay, Paris, France. [20]Cardiology Department, Assistance Publique Hôpitaux de Paris, Pitie-Salpêtrière Hospital, Paris, France. [21]Department of Biology and Biological Engineering, Chalmers University of Technology, Gothenburg, Sweden. [22]Integromics Unit, Institute of Cardiometabolism and Nutrition, Paris, France. [23]Sorbonne Université, IRD, Unité de Modélisation Mathématique et Informatique des Systèmes Complexes, UMMISCO, Paris, France. [24]Department of Pharmacology, Sorbonne Université, INSERM CIC-1901, UNICO-GRECO Cardio-oncology ProgramAP-HP.Sorbonne, Pitié-Salpêtrière Hospital, Assistance Publique-Hôpitaux de Paris, Paris, France. [25]Department of Cardiology, Rigshopitalet, University of Copenhagen, Copenhagen, Denmark. [26]Department of Clinical Biochemistry, Rigshopitalet, University of Copenhagen, Copenhagen, Denmark. [27]Department of Medicine, Bornholms Hospital, Rønne, Denmark. [28]Biobyte Solutions, Heidelberg, Germany. [29]Region Västra Götaland, Sahlgrenska University Hospital, Department of Clinical Physiology, Gothenburg, Sweden. [30]McGill University and Genome Quebec Innovation Centre, Montréal, Québec, Canada. [31]Section of Genomic and Environmental Medicine, National Heart & Lung Institute, Faculty of Medicine, Imperial College London, London, UK. [32]European Genomic Institute for Diabetes, CNRS UMR 8199, INSERM UMR 1283, Institut Pasteur de Lille, Lille University Hospital, University of Lille, Lille, France. [33]Helmholtz Institute for Metabolic, Obesity and Vascular Research (HI-MAG) of the Helmholtz Zentrum München, University of Leipzig, Leipzig, Germany. [34]Department of Bioinformatics, Biocenter, University of Würzburg, Würzburg, Germany. [35]Yonsei Frontier Lab (YFL), Yonsei University, Seoul, South Korea. [43]These authors contributed equally: Sofia K. Forslund, Rima Chakaroun, Maria Zimmermann-Kogadeeva, Lajos Markó, Judith Aron-Wisnewsky, Trine Nielsen. ✉e-mail: karine.clement@inserm.fr; michael.stumvoll@medizin.uni-leipzig.de; peer.bork@embl.org

The MetaCardis Consortium

Chloe Amouyal[8,28], Ehm Astrid Andersson Galijatovic[10], Fabrizio Andreelli[8,9,28], Olivier Barthelemy[20], Jean-Paul Batisse[20], Eugeni Belda[22], Magalie Berland[19], Randa Bittar[36], Hervé Blottière[19], Frederic Bosquet[28], Rachid Boubrit[20], Olivier Bourron[28], Mickael Camus[19], Dominique Cassuto[9], Cecile Ciangura[9,28], Jean-Philippe Collet[20], Maria-Carlota Dao[8], Morad Djebbar[20], Angélique Doré[19], Line Engelbrechtsen[8], Soraya Fellahi[12,13], Sebastien Fromentin[19], Pilar Galan[15], Dominique Gauguier[30,37], Philippe Giral[38], Agnes Hartemann[28], Bolette Hartmann[10], Jens Juul Holst[10], Malene Hornbak[10], Lesley Hoyles[39], Jean-Sebastien Hulot[24,40,41], Sophie Jaqueminet[19], Niklas Rye Jørgensen[28], Hanna Julienne[19], Johanne Justesen[10], Judith Kammer[7], Nikolaj Krarup[10], Mathieu Kerneis[20], Jean Khemis[9], Ruby Kozlowski[15], Véronique Lejard[20], Florence Levenez[20], Lea Lucas-Martini[9], Robin Massey[20], Laura Martinez-Gili[14], Nicolas Maziers[19], Jonathan Medina-Stamminger[9], Gilles Montalescot[20], Sandrine Moute[23], Ana Luisa Neves[15], Michael Olanipekun[15,31], Laetitia Pasero Le Pavin[19], Christine Poitou[8,9], Francoise Pousset[20], Laurence Pouzoulet[38], Andrea Rodriguez-Martinez[15], Christine Rouault[8], Johanne Silvain[20], Mathilde Svendstrup[10], Timothy Swartz[8,22,42], Thierry Vanduyvenboden[19], Camille Vatier[9] & Stefanie Walther[7]

[36]Biochemistry Department of Metabolic Disorders, Assistance Publique Hôpitaux de Paris, Pitie-Salpêtrière Hospital, Paris, France. [37]UMRS 1124 INSERM, Université de Paris Descartes, Paris, France. [38]Assistance Publique Hôpitaux de Paris, Endocrinology Department, Pitie-Salpêtrière Hospital, Paris, France. [39]Department of Biosciences, Nottingham Trent University, Nottingham, UK. [40]PARCC, INSERM, Université de Paris, Paris, France. [41]Assistance Publique Hôpitaux de Paris, Hôpital Européen Georges-Pompidou, CIC1418 and DMU CARTE, Paris, France. [42]Integrative Phenomics, Paris, France.

Methods

Study cohort and sample acquisition

The prospective cross-sectional multi-centre study MetaCardis covered a wide range of metabolic and cardiac phenotypes. For the purpose of the study a total of 2,173 individuals, including healthy individuals as well as individuals with increasingly severe metabolic and cardiac disease, were recruited into eight study groups in Denmark, Germany and France (Supplementary Table 1). Individuals were evaluated for suitability according to standardized inclusion and exclusion criteria across the three sites. Exclusion criteria included a past history of abdominal malignancy/intestinal resection/radiation, chronic or acute inflammatory disease, autoimmune disease, history of organ transplantation with immunosuppressive drug intake, severe kidney disease as defined by estimated glomerular filtration rate < 50 ml min^{-1} per 1.73 m^2, specific exclusion criteria allowed for a group-dependent specific phenotype acquisition. The study complied with all of the relevant international and respective local regulations and aligned with the declaration of Helsinki. The study protocol was approved by the Ethics Committee at the Medical Faculty at the University of Leipzig (application number: 047-13-28012013), the ethical committees of the Capital Region of Denmark (H-3-2013-145) and the ethics committee 'Comite de Protection des Personnes' (CPP) Ile-de-France III no. IDRCB2013-A00189-36. The study protocol was registered at https://clinicaltrials.gov/ (NCT02059538). All of the participants provided written informed consent. Sample size was not calculated prior to recruitment but was set to surpass earlier studies showing significant effect sizes of drug treatment on microbial gut signatures. Due to the nature of the study, randomization and blinding were not applied.

Groups were defined along international definitions of disease, with obesity defined according to the WHO criteria[31], metabolic syndrome according to the International Diabetes Federation[32], T2D by the American Diabetes Association[33] and hypertension according to the American College of Cardiology and American Heart Association[34]. For obesity specifically, participants were recruited into two groups: group 2A, consisting of individuals with mostly severe obesity (referred to in text as 2A: severe obesity), none of whom had T2D or previous cardiovascular conditions, whereas group 2B consisted of mostly individuals with morbid obesity, who were eligible for bariatric surgery (referred to in text as 2B: morbid obesity). T2D was not an exclusion criterion for this particular group (as compared with group 2A) and patients had overall more severe metabolic impairment (Supplementary Table 1). Individuals with heart failure were defined according to the American College of Cardiology, American Heart Association and the Heart Failure Society of America[35].

Phenotyping was performed according to standardized operational procedures between countries and included biological samples acquisition and anthropometrics, such as weight, height, body mass index calculation (BMI), blood pressure measurement and body composition analyses using bioimpedance analysis as well as waist and hip circumference measurements.

Participants answered questionnaires relating to medical and family history, physical activity, quality of life, eating behaviour as well as food intake using a customized validated food frequency questionnaire[36]. Medication/drug intake was assessed either by direct recall or by medication list when provided, and participants were questioned on adherence to the medication plan by an experienced clinician. Five-year antibiotics intake was assessed by recall in France and Denmark, whereas participants in Germany were requested to provide medication anamnesis from their general practitioners or physicians they were prescribed medications by in the past 5 years.

Cardiometabolic drugs were classified according to indication/category and further subdivided by drug class (Supplementary Table 4), aiming to resolve the major mechanisms of action at a granularity enabling statistical testing. All medication data were curated jointly by the study physicians at each centre so as to harmonize representation.

Blood samples were collected through standard venepuncture after an overnight fast and were used to assess metabolic markers in local routine laboratories. Analyses of adipokines, measures of insulin and C-peptide, inflammatory markers, free fatty acids and metabolomics were centralized at Pitié-Salpêtrière hospital. Plasma and serum samples were stored at the respective clinical centres at −80 °C until shipment to a central measuring facility. Stool samples were obtained by each participant at home and were immediately frozen. Frozen samples were then delivered to the respective study centres within 48 h on dry ice and were stored immediately at −80 °C until analysis. Fasting plasma glucose, total and HDL cholesterol, triglycerides, creatinine and HbA1c levels were measured using enzymatic methods at local laboratories in each centre according to benchmarked standardized methods. LDL cholesterol concentrations were measured enzymatically for German participants, and values for French and Danish participants were calculated on the basis of the Friedwald equation. Kinetic assays based on coupled enzyme systems were used to measure alanine aminotransferase (ALAT), aspartate aminotransferase (ASAT) and γ-glutamyltransferase (GGT) levels. Ultrasensitive C-reactive protein (usCRP) was measured using an Image Automatic Immunoassay System (Beckman Coulter). High-sensitivity IL-6 was measured using the Human IL-6 Quantikine HD ELISA Kit (R&D Systems). IFNγ-induced protein 10 (IP-10) and C-X-X motif chemokine ligand 5 (CXCL5), CCL2, eotaxin, IL-7, MIF, MIP1b, SDF1 and VEGFa were measured using the Luminex assay (ProcartaPlex Mix&Match Human 13-plex; eBioscience).

Data acquisition and preprocessing

Total faecal DNA from 1,901 individuals was extracted according to the International Human Microbiome Standards (IHMS) guidelines (SOP 07 V2 H) and sequenced using ion-proton technology (Thermo Fisher Scientific) resulting in 23.3 ± 4.0 million (mean ± s.d.) 150 bp single-end reads per sample on average. Reads were cleaned using Alien Trimmer (v.0.2.4)[37] to remove resilient sequencing adapters and trim low-quality nucleotides at the 3′ side (quality and length cut-off of 20 and 45 bp, respectively). Cleaned reads were subsequently filtered from human and potential food contaminant DNA (using human genome RCh37-p10, *Bos taurus* and *Arabidopsis thaliana* with an identity score threshold of 97%).

Gene abundance profiling was performed using the 9.9 million gene integrated reference catalogue of the human microbiome[38]. Filtered high-quality reads were mapped with an identity threshold of 95% to the 9.9-million-gene catalogue using Bowtie (v.2.2.6) included in the METEOR (v.3.2) software[39]. A gene abundance table was generated using a two-step procedure with METEOR. First, the uniquely mapping reads (reads mapping to a single gene in the catalogue) were attributed to their corresponding genes. Second, shared reads (reads that mapped with the same alignment score to multiple genes) were attributed according to the ratio of their unique mapping counts. The gene abundance table was processed for rarefaction and normalization and further analysis using the MetaOMineR[40] (v.1.2) R package. To decrease technical bias due to different sequencing depth and avoid any artefacts of sample size on low abundance genes, read counts were rarefied. The gene abundance table was rarefied to 10 million reads per sample by random sampling of 10 million mapped reads without replacement. The resulting rarefied gene abundance table was normalized according to the FPKM strategy (normalization by the gene size and the number of total mapped reads reported in frequency) to give the gene abundance profile table. Metagenomic species (MGS; co-abundant gene groups with more than 500 genes corresponding to microbial species; n = 1,436) were clustered from 1,267 human gut metagenomes used to construct the 9.9-million-gene catalogue[41]. MGS abundances were estimated as the mean abundance of the 50 genes defining a robust centroid of the cluster (if more than 10% of these genes gave positive signals). MGS taxonomical annotation was performed using all genes by sequence similarity using NCBI blastN; a species-level assignment

was given if >50% of the genes matched the same reference genome of the NCBI database (November 2016 version) at a threshold of 95% of identity and 90% gene length coverage. Remaining MGS were assigned to a given taxonomical level from genus to superkingdom if more than 50% of their genes had the same level of assignment. Microbial gene richness (gene count) was calculated by counting the number of genes that were detected at least once in a given sample, using the average number of genes counted in ten independent rarefaction experiments. Moreover, a second approach was used to quantify microbial taxa based on the mOTU approach[42]. The quantification of mOTU abundance per metagenome was performed according to the original methodology: (1) short reads were mapped to the database of single-copy marker genes;[42] (2) gene-level abundance tables were computed, normalizing by the size of each gene and the number of input reads, emulating the scaled mode in MOCAT2 (ref. [43]); (3) within each metagenome, the abundance of all reads mapping to genes within the same mOTU cluster and the same orthologous group (COG), was added together to obtain a mOTU–COG abundance table, emulating the functional mapping of MOCAT2 (ref. [43]) (which could not be used directly as the file formats were not appropriate); (4) this abundance table was then run through the final step in the NGLess interface[44] (v.1.3.0) to the mOTU tool to obtain the mOTU abundance table (in brief, the abundance of a mOTU is defined as the mean of its constituent COGs, while ignoring non-detected COGs, provided that at least two COGs have been detected, as in the original publication). For quantification of functional modules, metagenome reads mapped to the IGC gene catalogue after rarefaction to 10 million reads per sample were binned by functional category, as per the annotations of the previously analyses within the MOCAT2 framework[43]. Functional potentials at each class of annotations (such as KEGG modules) were summed within each annotation term.

Determination of faecal microbial load

Microbial loads of faecal samples were determined as described previously[11]. In brief, 0.2 g frozen (−80 °C) aliquots were dissolved in physiological solution (9 g l^{-1} NaCl; Baxter) to a total volume of 100 ml (8.5 g l^{-1} NaCl; VWR). Subsequently, the slurry was diluted 1,000 times. Samples were filtered using a sterile syringe filter (pore size of 5 µm; Sartorius Stedim Biotech). Next, 1 ml of the microbial cell suspension obtained was stained with 1 µl SYBR Green I (1:100 dilution in DMSO; shaded 15 min incubation at 37 °C; 10,000 concentrate, Thermo Fisher Scientific). The flow cytometry analysis was performed using a C6 Accuri flow cytometer (BD Biosciences)[45]. Fluorescence events were monitored using the FL1 533/30 nm and FL3 >670 nm optical detectors. Forward- and sideward-scattered light was also collected. The BD Accuri CFlow (v.1.0.264.21) software was used to gate and separate the microbial fluorescence events on the FL1/FL3 density plot from the faecal sample background. A threshold value of 2,000 was applied on the FL1 channel. The gated fluorescence events were evaluated on the forward/sideward density plot, as to exclude remaining background events. Instrument and gating settings were kept identical for all of the samples (fixed staining/gating strategy[45]; Extended Data Fig. 8). On the basis of the exact weight of the aliquots analysed, cell counts were converted to microbial loads per gram of faecal material.

Quantitative microbiome profiling

Phylogenetic quantitative microbiome profiles were built using a modified version of the pipeline described in Vandeputte et al.[46] (https://github.com/raeslab/QMP/). In short, sample abundance profiles were downsized to even sampling depth, defined as the ratio between the sample's sampling size (microbial cells sequenced) and microbial load (total microbial cell count). In 16S amplicon sequencing, sampling size is defined as total sequencing depth, whereas, for shotgun metagenomics, it is defined as the average mOTU marker genes coverage[43]. For both, microbial load is determined by flow cytometry as the average total cell count per gram of frozen faecal material. The sequencing depth of each sample was rarefied to the level necessary to equate the minimum observed sampling depth in the cohort. The rarefied mOTU abundance matrix was converted into numbers of cells per gram and quantitative microbiome profiling matrices created for phylum to species levels. Functional quantitative microbiome profiles and quantitative coabundance gene groups[41] profiles were constructed by multiplication of relative proportions to an indexing factor proportional to the microbial cell densities of the samples (load), defined as the sample load divided by the median load over the entire MetaCardis cohort.

Multivariate effects of antibiotics and non-antibiotic drugs

The multivariate effects of antibiotics and non-antibiotic drugs on microbiome and host metabolite features were tested. Only patients and healthy individuals with complete microbiome and host metabolomic features were considered. Variables with less than ten non-zero occurrences were excluded. Furthermore, variables were checked for high association using Kendall's tau correlation for correlations between pairs of numerical variables, intraclass correlation coefficient for pairs of numerical versus categorical variables, and Cramer's *V* for pairs of categorical variables. The variables 'PPI and related drugs' and 'TRIMETHOPRIM' were removed from the downstream analysis due to their high association (>0.8 correlation) with other variables. The threshold of 0.8 was chosen as it is the standard in the field[12,47]. Finally, non-antibiotic drugs and antibiotics to be tested were selected for each microbiome feature set as well as for the set of host phenotype measurements. This was achieved by automatic stepwise model building in both directions based on the Akaike information criterion, using the function ordistep in vegan package (v.2.4-5). The function chooses a model by permutation tests under constrained ordination, in this case, distance-based redundancy analysis (dbRDA) constructed on Bray–Curtis dissimilarities of square-root transformed values from each feature set. The variables selected were added to the set of control variables to compose the full models for each feature set. The control variables were selected on the basis of their potential confounding effects. Those were BMI, sex, age, country of recruitment, stool consistency (Bristol scale), alternative healthy eating index (as a measure of diet quality), smoking status and patient group (that is, disease categories or control status).

The unique effect of a given variable was assessed considering all of the other variables present in the model specific to each feature set. As in the model selection stage, dbRDA was constructed on Bray–Curtis dissimilarities of square-root transformed values from each feature set. The proportion of variation explained by a given variable independent of the other variables was obtained using the Condition function of the dbRDA implementation in the vegan R package (v.2.4-5). For each variable of interest, a new model was constructed by including all other variables within the Condition function. Type III analysis of variance was used to test significance of models with 999 permutations. *P* values were corrected for multiple testing using the Benjamini–Hochberg procedure. Adjusted *P* values of less than 0.05 were considered to be significant. Adjusted R^2 was recovered from the function using the vegan R function RsquareAdj. Adjusted R^2 was also obtained from the full model, that is, the model constructed without the Condition function. All calculations were performed in the R environment v.3.4.3 using the vegan package v.2.4-5. The code for multivariate analysis is documented and available under https://doi.org/10.5281/zenodo.4719526.

Univariate effects of antibiotics and non-antibiotic drugs

To assess the relative roles of drugs versus the disease influence on each microbiome or host measurement separately, a software pipeline was established according to the approach outlined in Extended Data Fig. 1. The approach followed hinges on filtering each naive association by the outcomes of post hoc tests for the influence of each salient covariate. In the first step, all of the tested features (separately by feature space, such as serum metabolites or gut microbial species) are checked for associations both for all group comparisons (that is, controls versus

each patient group for a case–control study such as MetaCardis) and for each potential covariate, for example, medicated versus unmedicated individuals for each drug or drug combination. This test is a two-sided Mann-Whitney *U*-test for binary variables, Kruskal–Wallis test for other categorical variables or a Spearman test for continuous variables. These tests are adjusted for multiple testing using Benjamini–Hochberg correction, with standardized effect sizes computed for binary variables using the Cliff's Delta metric (as implemented in the orddom R package (v.3.1)) and Spearman's ρ for continuous variables. These tests are conducted stratified for patient groups, separate for each, for every continuous non-constant variable and every binary variable where at least ten individuals in a patient group fall within each level of the variable. For the variable 'study center', which is the one nonbinary categorical variable tested, we performed the tests in every case. For each (continuous) feature, if a covariate is significant (FDR < 0.1) and relevant (absolute standardized effect size > 0.1, requirement omitted for study centre) in at least one patient group, then it is tested for in the post hoc test for all of the patient groups. The post hoc test is a nested linear model comparison test, where the feature, rank-transformed, is modelled using either both the tested variable (for example, drug or disease group comparison) and each other covariate in turn, versus a model containing only the covariate. The inverse test is also performed, comparing the more complex model to the one containing only the tested variable. *P* values for these models are computed using a likelihood ratio test for the models using the R lmtest package (v.0.9-38). If the model for the tested variable always retains a significantly (post-hoc $P < 0.05$) better fit than the covariate-only model omitting it, or if no salient covariates exist, the feature is considered to be associated under confident deconfounding with regards to the tested variable. If one or more covariates exist for which including the tested variable in the model does not significantly improve the model fit, but the same condition holds inversely for all such covariates, then the tested feature co-occurs so strongly with each salient covariate that it is not possible to assess whether the observed effect stems from the tested feature or the covariate; such a feature is considered to be ambiguously associated both with the tested variable and the covariates. Note also that it is possible for a feature to be associated even under confident deconfounding with several tested variables/covariates. If for a given feature its dependence on a tested variable is reducible to at least one covariate that in turn cannot be reduced to the influence of the tested variable, the effect of the tested variable on the feature is considered to be confounded by all such features. This classification therefore results in a set of feature–variable associations that are either confidently or ambiguously deconfounded, and in a similar map of the deconfounded associations of each possible covariate, tested separately in each patient group in MetaCardis where a naive effect can be observed and tested. Note that confidently deconfounded can be stated only within the scope of available metadata.

For the hierarchical clustering of drug associations with the host and microbiome features, the number of features of a specific type affected by each drug falling into each category was used to cluster the drug effects. Pearson's correlation was used as a distance metric for clustering.

Enrichment of oral strain populations in faecal samples

To quantify the differential faecal enrichment of oral strain populations, we relied on the multisite metagenomic dataset provided by the Human Microbiome Project (HMP) to define predominantly oral microbial single nucleotide variants (SNV). Raw sequence reads for 399 stool and 945 oral HMP samples (from 9 distinct subsites) were downloaded from the European Nucleotide Archive (ENA: PRJNA48479, PRJNA275349), quality-trimmed and mapped to reference genomes of 1,753 specI clusters[42] using NGlessR[44] (v.1.3.0). Uniquely mapping reads for all oral subsites were then combined per individual and time point into a total of 375 oral samples, using the samtools merge command. Faecal samples for the present cohort were processed in a similar manner and mapped to the same set of specI reference genomes.

For the resulting combined dataset, microbial SNVs were called using metaSNV[48] (v.1), requiring a minimum of 4 non-reference reads at a prevalence of ≥5% of total samples to define an SNV. From the resulting set, all SNVs observed in at least half of oral HMP samples and at least 10 HMP faecal samples were defined as predominantly oral and used as proxies to quantify oral microbial strain populations in MetaCardis faecal samples. By using the threshold on the lowest number of faecal samples (at least 10), we selected strains that are predominantly linked to the oral cavity, but which can at least sometimes be observed in the gut as well, which enabled us to make the test more conservative and ensure robustness to noise.

Medication intake and co-prescription frequency

To infer association rules for drug co-prescription rules, the Equivalence Class Transformation algorithm implemented in the R library arules[49] (v.1.6-2) was used. Drug effects against disease were calculated according to the univariate tests described above; effects that had the opposite direction to those found comparing patients versus controls were considered to be putative drug effects, whereas effects that had the same sign as the disease signature were putatively labelled as severity markers or indications for receiving a drug for purposes of visualization. Plots were generated using ggptlot2, ggpubr and igraph R libraries, using R v.3.5.3.

Mediation analysis

To assess whether drug effects on the host features were mediated by changes in the microbiome features or vice versa, we performed general mediation analysis[50] implemented in the Python (v.3.7.7) library statsmodels[51] (v.0.11.0). For each drug or drug combination, we included only host and microbiome features that were associated with the treatment with the single drug, drug dosage or the drug combination, correspondingly. The thresholds for association were (1) MWU FDR < 0.1; (2) passing all confounder filters; (3) disease association is the opposite in direction to that of the drug combination; and (4) in the case of dosage and combination, significance in a nested linear model comparison test (likelihood ratio post hoc $P < 0.05$). The basic mediation analysis was performed using the formulas feature ~ drug + mediator for the outcome model (defined with the function sm.GLM.from_formula) and mediator ~ drug for the mediator model (defined with a function sm.OLS.from_formula). The effect size and significance of mediation was calculated with the function statsmodels.stats.mediation.Mediation.fit() using 'drug' and 'mediator' as parameters. In addition to mediation analysis, we also calculated the Pearson's correlation between each feature and each mediator included in the analysis for each effector.

Reporting summary

Further information on research design is available in the Nature Research Reporting Summary linked to this paper.

Data availability

The source data for the figures are provided at Zenodo (https://doi.org/10.5281/zenodo.4728981). Raw shotgun sequencing data that support the findings of this study have been deposited at the ENA under accession codes PRJEB41311, PRJEB38742 and PRJEB37249 with public access. Raw spectra for metabolomics have been deposited in the MassIVE database under the accession codes MSV000088043 (UPLC–MS/MS) and MSV000088042 (GC–MS). The metadata on disease groups and drug intake are provided in Supplementary Tables 1–3. The demographic, clinical and phenotype metadata, and processed microbiome and metabolome data for French, German and Danish participants are available at Zenodo (https://doi.org/10.5281/zenodo.4674360).

Code availability

The new drug-aware univariate biomarker testing pipeline is available as an R package (metadeconfoundR; Birkner et al., manuscript in preparation) at Github (https://github.com/TillBirkner/metadeconfoundR) and at Zenodo (https://doi.org/10.5281/zenodo.4721078). The latest version (0.1.8) of this package was used to generate the data shown in this publication. The code used for multivariate analysis based on the VpThemAll package is available at Zenodo (https://doi.org/10.5281/zenodo.4719526). The phenotype and drug intake metadata, processed microbiome, and metabolome data and code resources are available for download at Zenodo (https://doi.org/10.5281/zenodo.4674360). The code for reproducing the figures is provided at Zenodo (https://doi.org/10.5281/zenodo.4728981).

31. Branca, F., Nikogosian, H. & Lobstein, T. The Challenge of Obesity in the WHO European Region and the Strategies for Response. Summary, https://www.euro.who.int/en/publications/abstracts/challenge-of-obesity-in-the-who-european-region-and-the-strategies-for-response-the.-summary (WHO, 2007).
32. Alberti, K. G. M. M., Zimmet, P. & Shaw, J. The metabolic syndrome–a new worldwide definition. *Lancet* **366**, 1059–1062 (2005).
33. Petersmann, A. et al. Definition, classification and diagnosis of diabetes mellitus. *Exp. Clin. Endocrinol. Diabetes* **127**, S1-S7 (2019).
34. Whelton, P. K. et al. 2017 ACC/AHA/AAPA/ABC/ACPM/AGS/APhA/ASH/ASPC/NMA/PCNA guideline for the prevention, detection, evaluation, and management of high blood pressure in adults: executive summary: a report of the American College of Cardiology/American Heart Association Task Force on clinical practice guidelines. *Hypertension* **71**, 1269–1324 (2018).
35. Yancy, C. W. et al. 2017 ACC/AHA/HFSA focused update of the 2013 ACCF/AHA guideline for the management of heart failure: a report of the American College of Cardiology/American Heart Association Task Force on clinical practice guidelines and the Heart Failure Society of America. *J. Card. Fail.* **23**, 628–651 (2017).
36. Verger, E. O. et al. Dietary assessment in the MetaCardis study: development and relative validity of an online food frequency questionnaire. *J. Acad. Nutr. Diet.* **117**, 878–888 (2017).
37. Criscuolo, A. & Brisse, S. AlienTrimmer: a tool to quickly and accurately trim off multiple short contaminant sequences from high-throughput sequencing reads. *Genomics* **102**, 500–506 (2013).
38. Li, J. et al. An integrated catalog of reference genes in the human gut microbiome. *Nat. Biotechnol.* **32**, 834–841 (2014).
39. Cotillard, A. et al. Dietary intervention impact on gut microbial gene richness. *Nature* **500**, 585–588 (2013).
40. Prifti, E. & Le Chatelier, E. MetaOMineR. A quantitative metagenomics data analyses pipeline v.hal-02800484 (2014).
41. Nielsen, H. B. et al. Identification and assembly of genomes and genetic elements in complex metagenomic samples without using reference genomes. *Nat. Biotechnol.* **32**, 822–828 (2014).
42. Sunagawa, S. et al. Metagenomic species profiling using universal phylogenetic marker genes. *Nat. Methods* **10**, 1196–1199 (2013).
43. Kultima, J. R. et al. MOCAT2: a metagenomic assembly, annotation and profiling framework. *Bioinformatics* **32**, 2520–2523 (2016).
44. Coelho, L. P. et al. NG-meta-profiler: fast processing of metagenomes using NGLess, a domain-specific language. *Microbiome* **7**, 84 (2019).
45. Prest, E. I., Hammes, F., Kötzsch, S., van Loosdrecht, M. C. M. & Vrouwenvelder, J. S. Monitoring microbiological changes in drinking water systems using a fast and reproducible flow cytometric method. *Water Res.* **47**, 7131–7142 (2013).
46. Vandeputte, D. et al. Quantitative microbiome profiling links gut community variation to microbial load. *Nature* **551**, 507–511 (2017).
47. Katz, M. H. *Multivariable Analysis. A Practical Guide for Clinicians and Public Health Researchers* (Cambridge Univ. Press, 2011).
48. Costea, P. I. et al. metaSNV: a tool for metagenomic strain level analysis. *PLoS ONE* **12**, e0182392 (2017).
49. Hahsler, M., Gruen, B., Hornik, K. arules–a computational environment for mining association rules and frequent item sets. *J. Stat. Softw.* **14**, 1–25. (2005).
50. Imai, K., Keele, L. & Tingley, D. A general approach to causal mediation analysis. *Psychol. Methods* **15**, 309–334 (2010).
51. Seabold, S. & Perktold J. statsmodels: econometric and statistical modeling with Python. In *Proc. 9th Python in Science Conference* (2010).
52. Palleja, A. et al. Recovery of gut microbiota of healthy adults following antibiotic exposure. *Nat. Microbiol.* **3**, 1255–1265 (2018).

Acknowledgements We thank the MetaCardis participants for their participation in the study, and particularly the patient associations (Alliance du Coeur and CNAO) for their input and interface; D. Bonnefont-Rousselot (Department of Metabolic Biochemistry, Pitié-Salpêtrière Hospital) for the analysis of plasma lipid profiles; and the nurses, technicians, clinical research assistants and data managers from the Clinical Investigation Platform at the Institute of Cardiometabolism and Nutrition for patient investigations, the Clinical Investigation Center (CIC) from Pitié-Salpêtrière Hospital and Human Research Center on Nutrition (CRNH Ile-de-France) as well as the university hospital of Leipzig for the investigation of healthy control individuals. Quanta Medical provided regulatory oversight of the clinical study and contributed to the processing and management of electronic data. This work was supported by the European Union's Seventh Framework Program for research, technological development and demonstration under grant agreement HEALTH-F4-2012-305312 (METACARDIS). Part of this work was also supported by the EMBL, by the Metagenopolis grant ANR-11-DPBS-0001, by the H2020 European Research Council (ERC-AdG-669830) (to P.B.), and by grants from the Deutsche Forschungsgemeinschaft (SFB1365 to S.K.F. and L.M.; and SFB1052/3 A1 MS to M.S. (209933838)). Assistance Publique-Hôpitaux de Paris is the promoter of the clinical investigation (MetaCardis). M.-E.D. is supported by the NIHR Imperial Biomedical Research Centre and by grants from the French National Research Agency (ANR-10-LABX-46 (European Genomics Institute for Diabetes)), from the National Center for Precision Diabetic Medicine – PreciDIAB, which is jointly supported by the French National Agency for Research (ANR-18-IBHU-0001), by the European Union (FEDER), by the Hauts-de-France Regional Council (Agreement 20001891/NP0025517) and by the European Metropolis of Lille (MEL, Agreement 2019_ESR_11) and by Isite ULNE (R-002-20-TALENT-DUMAS), also jointly funded by ANR (ANR-16-IDEX-0004-ULNE), the Hauts-de-France Regional Council (20002845) and by the European Metropolis of Lille (MEL). R.J.A. is a member of the Collaboration for joint PhD degree between EMBL and Heidelberg University, Faculty of Bioscience. The Novo Nordisk Foundation Center for Basic Metabolic Research is an independent research institution at the University of Copenhagen partially funded by an unrestricted donation from the Novo Nordisk Foundation.

Author contributions K.C. (coordinator), P.B., M.S., O.P., S.D.E., J.R., M.-E.D., F.B. and J.N. conceived the overall objectives and study design of the MetaCardis initiative. S.K.F. and P.B. developed the present project concept and protocol and supervised the project. MetaCardis cohort recruitment, phenotyping and lifestyle recording were conducted by R.C., J.A.-W., T.N., C.L., L.K., T.H., T.H.H., H.V. and K.A., and supervised by M.S., K.C. and O.P. Data curation was undertaken by S.K.F., R.C., L.M., K.A., J.A.-W. and T.N.. Faecal microbial DNA extraction and shotgun sequencing was performed by N.P., E.L.C. and S.F. Bacterial cell count measurement was performed by G.F. and S.V.-S. Serum and urine metabolome profiling was performed by L.H., J.C., A.M. and M.O. Bioinformatics and statistical analyses were performed by T.B., M.Z.-K., S.K.F., L.S., T.S.B.S., L.P.C., N.S., J.Z., E.P., S.F., R.C., S.V., G.F. and B.J. The manuscript was drafted by S.K.F., R.C., M.Z.-K. and L.M. All of the authors participated in the project development, revision of Article and approved the final version for publication.

Competing interests F.B. is shareholder in Implexion Pharma AB. K.C. is a consultant for Danone Research, LNC therapeutics and CONFO therapeutics for work that is unassociated with the present study. K.C. has held a collaborative research contract with Danone Research in the context of MetaCardis project. M.B. received lecture and/or consultancy fees from AstraZeneca, Boehringer-Ingelheim, Lilly, Novo Nordisk, Novartis and Sanofi. The other authors declare no competing interests.

Additional information

Supplementary information The online version contains supplementary material available at https://doi.org/10.1038/s41586-021-04177-9.

Correspondence and requests for materials should be addressed to Karine Clément, Michael Stumvoll or Peer Bork.

Peer review information *Nature* thanks Peter Turnbaugh and the other, anonymous, reviewer(s) for their contribution to the peer review of this work.

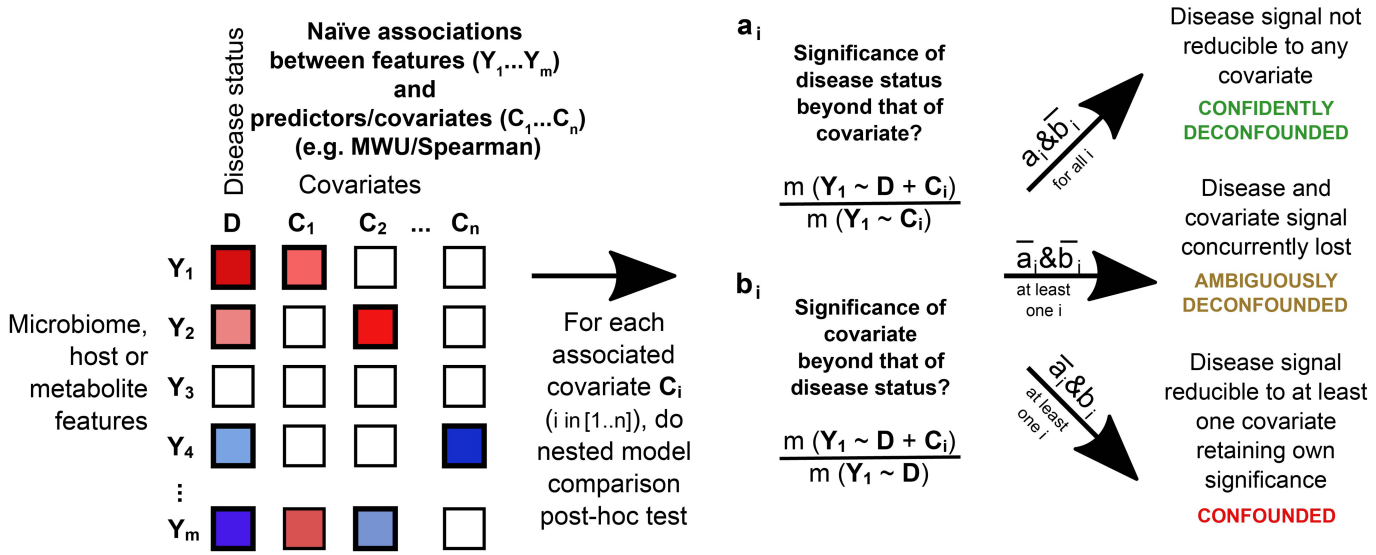

Extended Data Fig. 1 | A post-hoc testing approach for deconfounding univariate biomarker analysis for multiple medications and risk factors. The schematic highlights our covariate control approach. All significant associations between putative drivers (e.g., disease D) and covariates (C1...Cn) to each measured feature (Y1...Ym) are taken. The outcome of the test is denoted with a_i for a positive outcome ("yes") and $\bar{a}_i$ for a negative outcome ("no"). A significant predictor is called "confounded" and is filtered out in a post-hoc test if there is at least one covariate (e.g., drug treatment or combination) such that the predictor does not add significant predictive capacity beyond the covariate ("confounded"). If no such covariate itself passes the same test (i.e., covariates cannot in turn be shown to have predictive capacity beyond tested predictor), the predictor is considered ambiguous ("ambiguously deconfounded"). Otherwise, the predictor is considered "confidently deconfounded" (we note that "confidently deconfounded" is defined as no confounders were found among all covariates measured in our study).

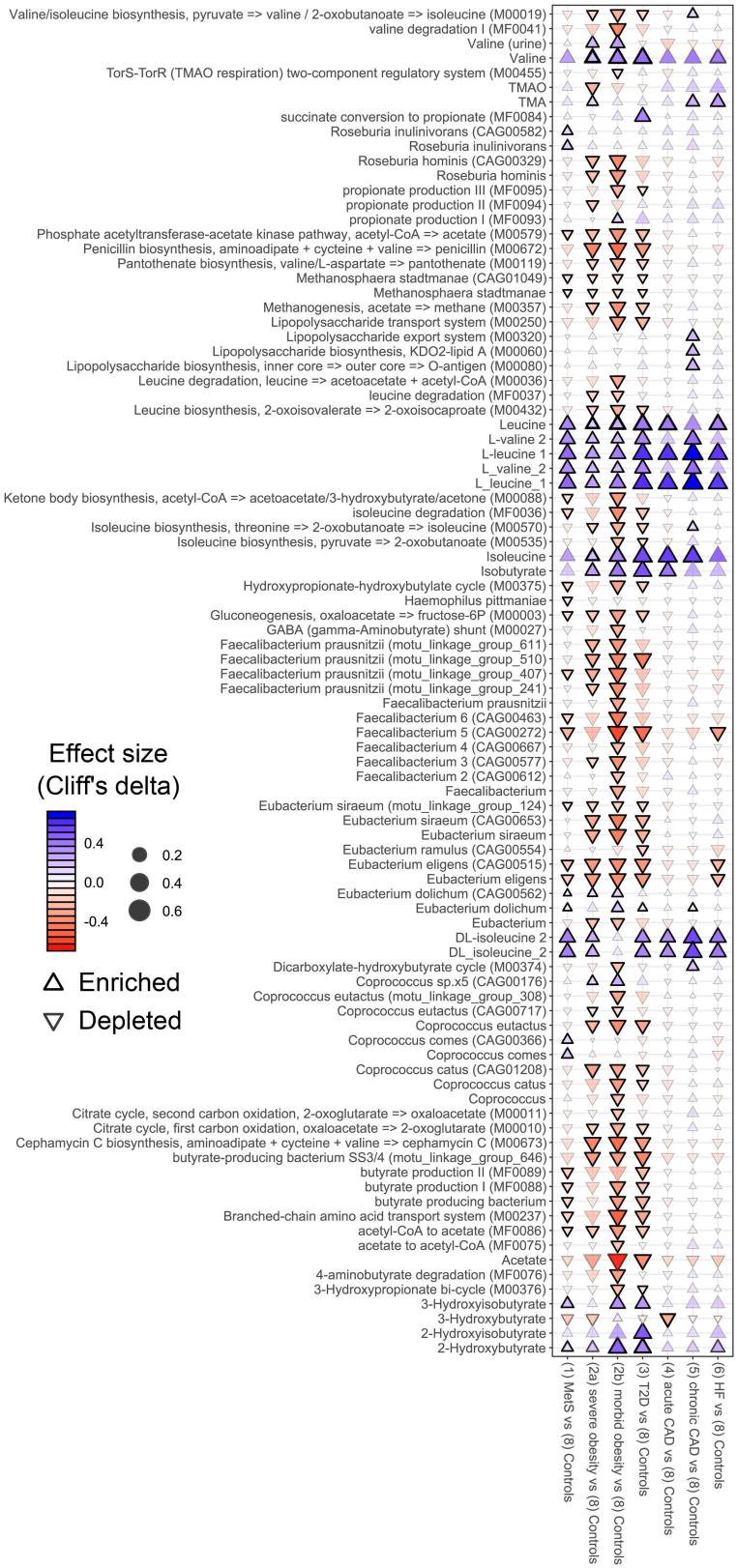

Extended Data Fig. 2 | Previously reported metabolic disease associations are replicated in the MetaCardis cohort under drug deconfounding, highlighting systemic inflammation, short-chain fatty acid and branched-chain amino acid mechanisms underlying insulin resistance. Cuneiform plot marker hues and direction show sign of effect size (Cliff's delta), intensity and size show amplitude of effect size, comparing metabolic diseased proband subsets (horizontal axis) with healthy control subject in the MetaCardis population for different microbiome, metabolome and host features (vertical axis). Bold and opaque markers show significant associations (two-sided MWU FDR < 0.1) not reducible to any significant drug or demographic confounder. Full associations are found in Supplementary Table 9; here a preselected subset is displayed reflecting previously reported risk and protective factors, validated in MetaCardis. ^{1}H NMR features are shown with retention time in parentheses, functional modules with GMM or KEGG identifier in parenthesis, analogous for metagenomic species and mOTUs.

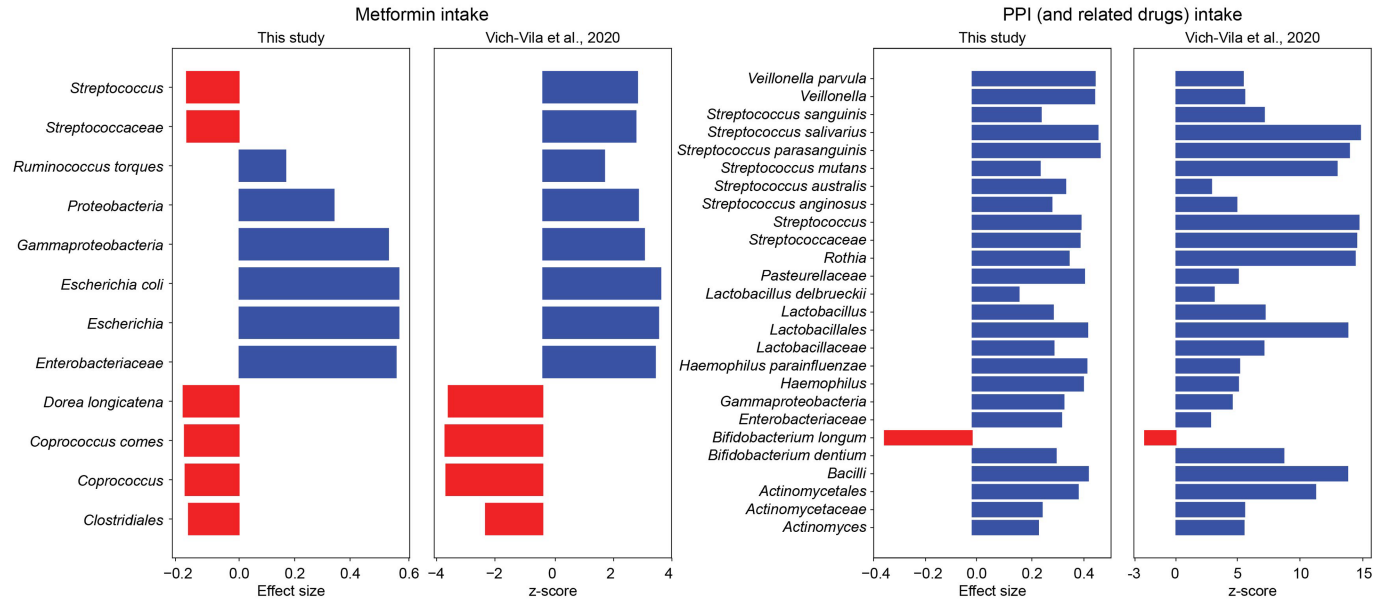

Extended Data Fig. 3 | Previously reported drug-microbiome associations are replicated in the MetaCardis cohort for metformin and PPI. Bar plots show the magnitude and direction of effect size (Cliff's delta) of metformin treatment (left) and PPI treatment (right) on microbiome features. These effects are compared to the previously published data from two independent patient cohorts[10]. Only features with direct match on the taxonomic level were included in the comparison. Full list of associations is provided in Supplementary Table 6.

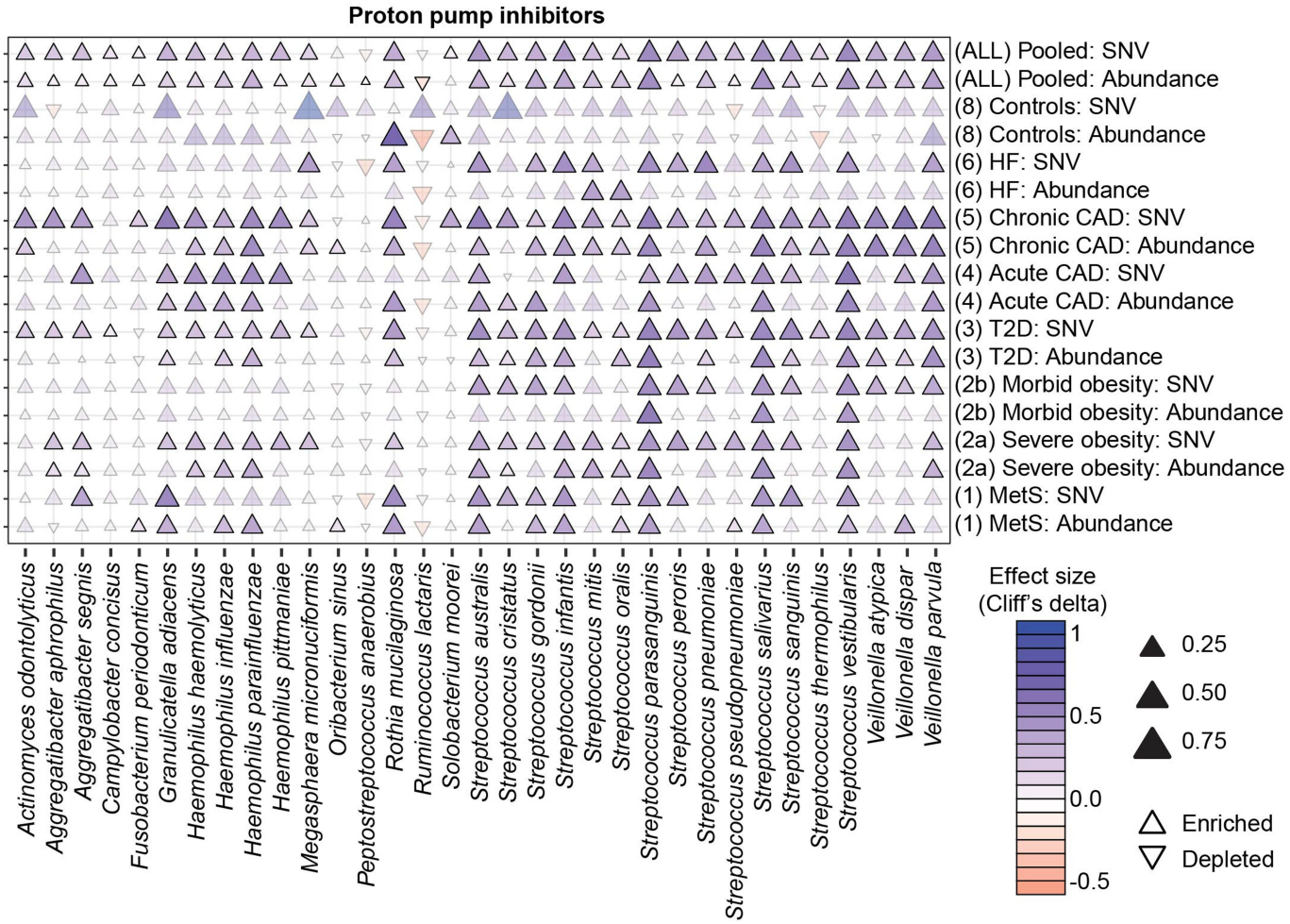

Extended Data Fig. 4 | SNV analysis of strains in the gut of subjects taking PPIs. Cuneiform plot shows change in abundance of bacterial species in the gut in subjects taking/not taking PPIs (controlling for other drugs and demographic factors) in each clinical group separately, and for all subjects pooled together. Rows marked "SNV" show whether oral strain single nucleotide markers are significantly (two-sided MWU FDR < 0.1) enriched over gut strain markers in subjects taking PPIs, controlling for abundance of each species. Marker direction, colour and size denote the sign and value of Cliff's delta standardized effect size; opaque markers are significantly altered (two-sided MWU FDR < 0.1; passing all confounder checks). Bacteria are shown if their abundance is significantly altered under PPI consumption, and there are SNPs distinguishing oral from gut strains in HMP samples. (See Supplementary Tables 5–7).

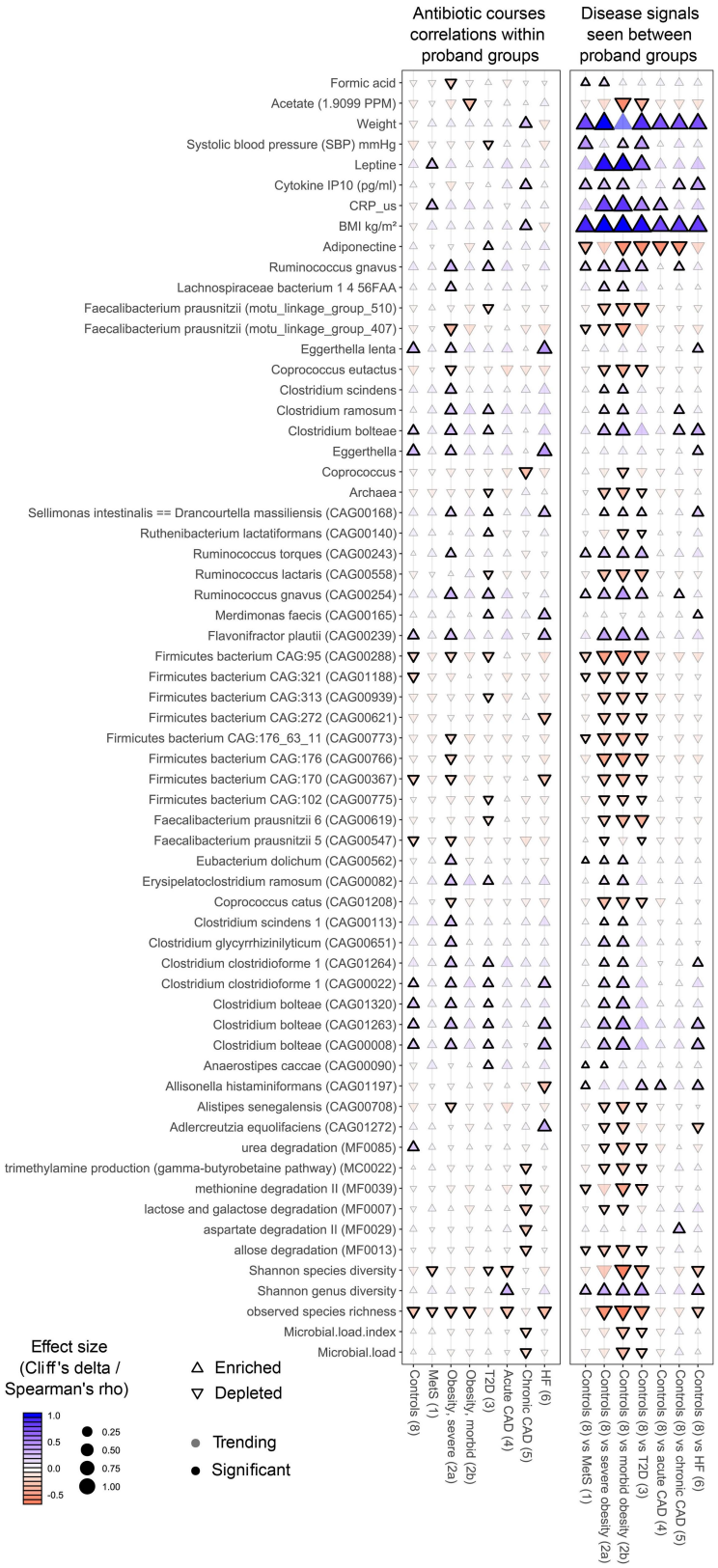

Extended Data Fig. 5 | Breakdown of antibiotics association into individual features, selected features shown. Left cuneiform plot (markers show Spearman correlation direction by shape and colour, scope by size and colour, significance (two-sided MWU FDR < 0.1, deconfounded for other drug and demographic features) by edge opacity) shows association between each feature and total number of antibiotics courses in CMD groups as well as in healthy controls. Right cuneiform shows whether the same features are significantly different (two-sided MWU FDR < 0.1) between healthy controls and CMD subjects following drug deconfounding (markers show Cliff's delta effect size), requiring significant and deconfounded correlation with number of antibiotic courses demonstrable in at least one proband group and at least one group showing significant and deconfounded alteration compared to healthy controls. Core features include increased carriage of possible disease-associated *Ruminococcus gnavus* and various *Clostridia* species, alongside decreased carriage of commensals such as *Faecalibacterium* species. Full list of associations is provided in Supplementary Table 12.

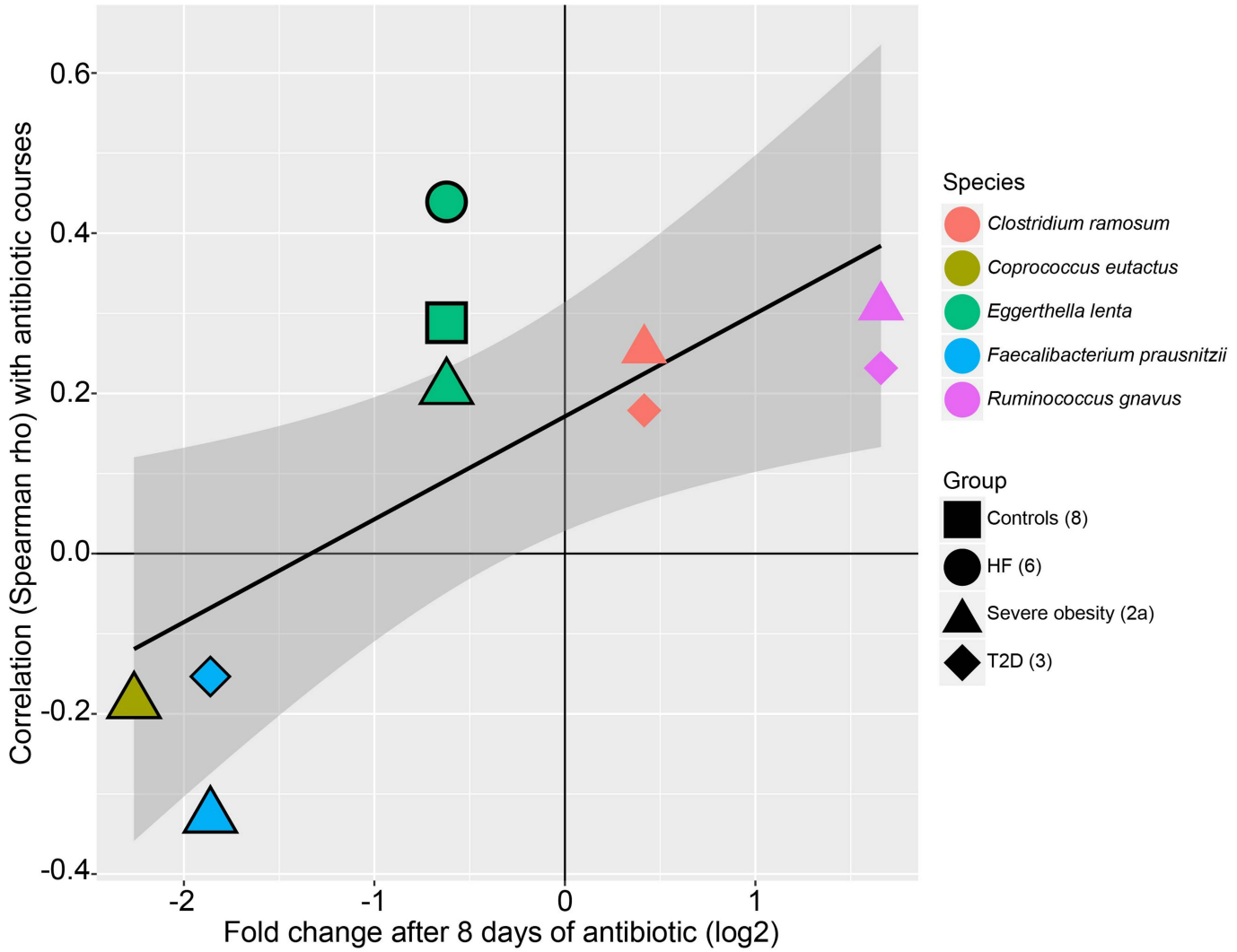

Extended Data Fig. 6 | Taxonomic changes are validated in a recent intervention cohort. For bacterial species where an effect on abundance of total antibiotics courses in MetaCardis could be demonstrated (significant at Spearman FDR < 0.1 and deconfounded), and where effect of antibiotic intervention has been tested in a recent antibiotic intervention study[52], MetaCardis correlation on vertical axis vs intervention log-transformed fold change on horizontal axis are displayed. Separate markers are shown for each MetaCardis patient group within which antibiotic effect can be demonstrated. Bold markers achieve significance (FDR < 0.1) in the intervention study as well. For the majority of taxa overlapping between studies, direction of changes matches, consistent with a causal impact of antibiotics on the microbiota in MetaCardis.

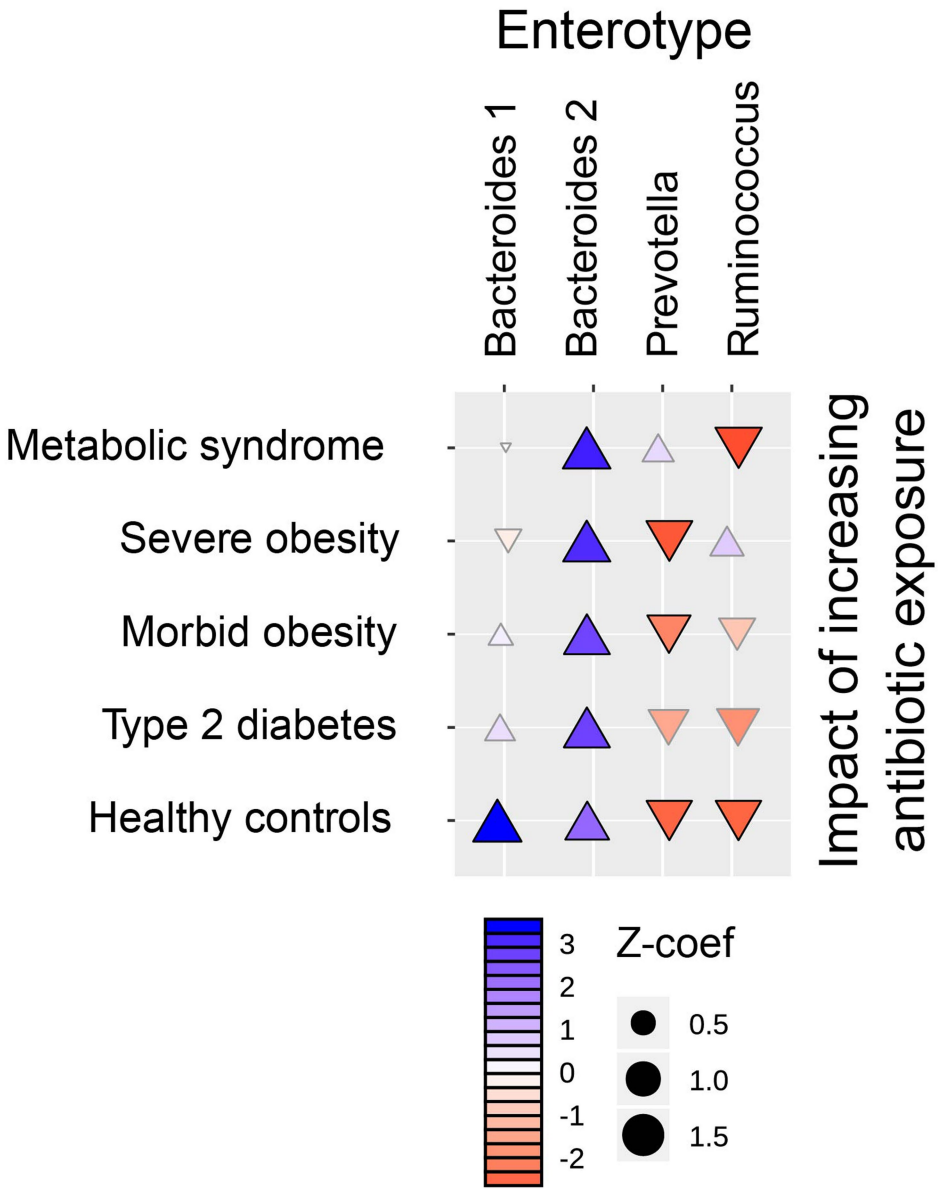

Extended Data Fig. 7 | Enterotype likelihood is altered by antibiotics. Cuneiform shows normalized regression coefficients of logistic models for each 4-class enterotype as a function of antibiotics courses in the past 5 years, separately for controls and metabolic disease patient groups. All significant (two-sided Wald FDR < 0.1) models show depletion of Ruminococcus and Prevotella enterotypes, and enrichment for Bacteroides enterotypes; in the case of metabolic disease patients, this is strongest for the low cell count Bacteroides 2 enterotype.

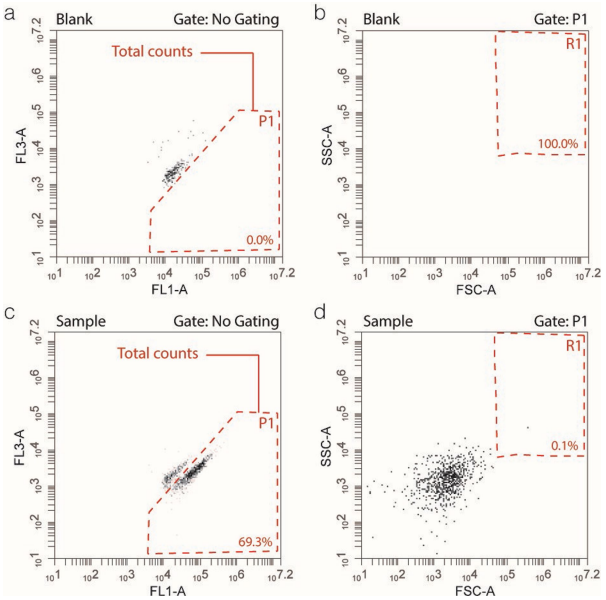

Extended Data Fig. 8 | Illustration of flow cytometry gating strategy. A fixed gating/staining approach was applied[45]. Both blank and sample solutions were stained with SYBR Green I. **a**. FL1-A/FL3-A acquisition plot of a blank sample (0.85% w/v physiological solution) with gate boundaries indicated. A threshold value of 2000 was applied on the FL1 channel. **b**. Secondary gating was performed on the FSC-A/SSC-A channels to further discriminate between debris/background and microbial events. **c**, **d**./ FL1-A/ FL3-A count acquisition of a faecal sample with secondary gating on FSC-A/ SSC-A channels based on blank analyses. Total counts were defined as events registered in the FL1-A/FL3-A gating area excluding debris/background events observed in the FSC-A/SSC-A R1 gate. The flow rate was set at 14 microliters per minute and the acquisition rate did not exceed 10,000 events per second. Each panel reflects the events registered during a 30 s acquisition period. Cell counts were determined in duplicate starting from a single biological sample.

nature research

Corresponding author(s): Peer Bork

Last updated by author(s): Sep 8, 2021

Reporting Summary

Nature Research wishes to improve the reproducibility of the work that we publish. This form provides structure for consistency and transparency in reporting. For further information on Nature Research policies, see our Editorial Policies and the Editorial Policy Checklist.

Statistics

For all statistical analyses, confirm that the following items are present in the figure legend, table legend, main text, or Methods section.

n/a	Confirmed	
☐	☒	The exact sample size (*n*) for each experimental group/condition, given as a discrete number and unit of measurement
☒	☐	A statement on whether measurements were taken from distinct samples or whether the same sample was measured repeatedly
☐	☒	The statistical test(s) used AND whether they are one- or two-sided *Only common tests should be described solely by name; describe more complex techniques in the Methods section.*
☐	☒	A description of all covariates tested
☐	☒	A description of any assumptions or corrections, such as tests of normality and adjustment for multiple comparisons
☐	☒	A full description of the statistical parameters including central tendency (e.g. means) or other basic estimates (e.g. regression coefficient) AND variation (e.g. standard deviation) or associated estimates of uncertainty (e.g. confidence intervals)
☐	☒	For null hypothesis testing, the test statistic (e.g. *F*, *t*, *r*) with confidence intervals, effect sizes, degrees of freedom and *P* value noted *Give P values as exact values whenever suitable.*
☒	☐	For Bayesian analysis, information on the choice of priors and Markov chain Monte Carlo settings
☒	☐	For hierarchical and complex designs, identification of the appropriate level for tests and full reporting of outcomes
☐	☒	Estimates of effect sizes (e.g. Cohen's *d*, Pearson's *r*), indicating how they were calculated

Our web collection on statistics for biologists contains articles on many of the points above.

Software and code

Policy information about availability of computer code

Data collection	For full details see Methods; METEOR (v3.2), MetaOMineR (v1.2), Alien Trimmer (v0.2.4) , MOCAT2 (v2.0), ngless (v1.3.0), Bowtie (v2.2.6), samtools (v1.13) were used to process microbiome data.
Data analysis	For full details see Methods; the following R packages were used: vegan (v2.4-5), lmtest (v0.9-38), orddom (v3.1), arules (v 1.6-2), ggplot2 (v3.3.4), ggpubr (v0.4.0) and igraph (v1.2.6). The following Python modules were used in Python (v3.7.7): numpy (v1.18.1), pandas (v1.0.3), scipy (v1.6.2), statsmodels (v0.11.0). Custom R code (metadeconfoundR pipeline (v0.2.1) and wrapper scripts to reproduce the results are available on github (https://github.com/TillBirkner/metadeconfoundR) and Zenodo (https://doi.org/10.5281/zenodo.4721078; https://doi.org/10.5281/zenodo.4719526; https://doi.org/10.5281/zenodo.4674360; https://doi.org/10.5281/zenodo.4728981)).

For manuscripts utilizing custom algorithms or software that are central to the research but not yet described in published literature, software must be made available to editors and reviewers. We strongly encourage code deposition in a community repository (e.g. GitHub). See the Nature Research guidelines for submitting code & software for further information.

Data

Policy information about availability of data

All manuscripts must include a data availability statement. This statement should provide the following information, where applicable:

- Accession codes, unique identifiers, or web links for publicly available datasets
- A list of figures that have associated raw data
- A description of any restrictions on data availability

Raw shotgun sequencing data that support the findings of this study have been deposited in The European Nucleotide Archive (ENA) with accession codes [PRJEB41311, PRJEB38742 and PRJEB37249] with public access. The metadata for all samples are provided in Supplementary Tables 2 and 3. The metadata, processed microbiome and metabolome data are available under https://doi.org/10.5281/zenodo.4674360 for download. The source data for the figures and

corresponding code are provided under https://doi.org/10.5281/zenodo.4728981. All data needed to replicate the results and figures in this manuscript are made available in the aforementioned resources.

Field-specific reporting

Please select the one below that is the best fit for your research. If you are not sure, read the appropriate sections before making your selection.

☒ Life sciences ☐ Behavioural & social sciences ☐ Ecological, evolutionary & environmental sciences

For a reference copy of the document with all sections, see nature.com/documents/nr-reporting-summary-flat.pdf

Life sciences study design

All studies must disclose on these points even when the disclosure is negative.

Sample size	No prior power calculation was carried out but sample size was selected so as to exceed that of the MetaHIT study, which was adequately powered.
Data exclusions	No subjects for which data was available was excluded during analysis.
Replication	As a hypothesis generating study, no explicit replication attempts were made, but 1) tests were performed separately in different participant groups, showing agreement; 2) previously published results were replicated in the present study. As stated in the manuscript, we could reproduce effects on serum metabolome of antidiabetic drugs, statins, beta-blockers, antithrombotic drugs and aspirin. Our approach recaptured previously reported drug-gut microbiome findings on the impact of antibiotics, PPIs, statins, beta-blockers and metformin. Specifically, for the study of Maier et al. Nature 2018 (https://doi.org/10.1038/nature25979), we reproduced at least one negative drug-microbial interactions for 6 out of 8 drugs overlapping between our studies (75%), which is summarized in Supplementary Table 6. For the study of Vich Vila et al. Nature Communications 2020 (https://doi.org/10.1038/s41467-019-14177-z), we could reproduce 10/12 (83%) of overlapping drug-microbiome interactions for metformin, and 26/26 (100%) of overlapping drug-microbiome interactions for proton pump inhibitors (summarized in Extended Data Figure 3).
Randomization	Since no intervention was performed, there was in principle nothing to randomize. However, wherever samples were processed in batch in the course of -omics data generation (including DNA extraction, sequencing, metabolomics measurements as well as preprocessing), they were randomly assigned to batches. Thus for all purposes that randomization is well-defined for this type of study design, it was carried out. We do not anticipate any resulting bias.
Blinding	Computational analysis was effectively blinded by default, as was processing of all data. Clinical laboratory measures and -omics data processing was likewise done blinded to the group labels (with samples given group-unrelated identifiers and labelled using derived barcode stickers), and with staff performing these procedures being unaware of sample group labels. The only data collection done by any staff aware of the group labels was initial clinical data collection by study nurses and physicians, who due to the design of the study (group labels reflecting diagnosis) cannot be blinded. We do not anticipate any resulting bias.

Reporting for specific materials, systems and methods

We require information from authors about some types of materials, experimental systems and methods used in many studies. Here, indicate whether each material, system or method listed is relevant to your study. If you are not sure if a list item applies to your research, read the appropriate section before selecting a response.

Materials & experimental systems

n/a	Involved in the study
☒	☐ Antibodies
☒	☐ Eukaryotic cell lines
☒	☐ Palaeontology and archaeology
☒	☐ Animals and other organisms
☐	☒ Human research participants
☐	☒ Clinical data
☒	☐ Dual use research of concern

Methods

n/a	Involved in the study
☒	☐ ChIP-seq
☐	☒ Flow cytometry
☒	☐ MRI-based neuroimaging

Human research participants

Policy information about studies involving human research participants

Population characteristics	This is described in detail within the manuscript as part of what we study, relative to both geographical, clinical, demographic and treatment factors (see Supplementary Table 1).
Recruitment	This is described in greater detail in the manuscript and companion manuscripts, and involve hospital regions of Paris, Copenhagen and Leipzig during period 2012-2016. Patients were recruited in the course of receiving specialist care in the

	participating clinics. Healthy controls were recruited through public advertisement in the cities where the clinics were located. Subjects recruited into the patient groups were selected according to the clinical group criteria. As such all patients fulfilling these criteria were asked to take part in the study and the return rate was above 90%. Healthy subjects in Germany were recruited via public advertisement, as it was not possible to randomly sample the population, so a slight selection bias can not be excluded for this particular group stemming from an overt interest in health. Considering this is beneficial for fidelity of study design when impacting specifically healthy controls, we can exclude that this impacted the results of the study. Moreover, the criteria for each group were overseen by recruiting physicians, leading to further filtering of groups. In summary, all subjects recruited with study groups were included upon preselection according to the group requirements and not upon interest of subject.
Ethics oversight	The study protocol was approved by the Ethics Committee at the Medical Faculty at the University of Leipzig, the Ethics Committees of the Capital Region of Denmark and the Ethics Committee CPP Ile-de-France. All participants provided written informed consent.

Note that full information on the approval of the study protocol must also be provided in the manuscript.

Clinical data

Policy information about clinical studies

All manuscripts should comply with the ICMJE guidelines for publication of clinical research and a completed CONSORT checklist must be included with all submissions.

Clinical trial registration	The study protocol was registered at ClinicalTrials.gov (NCT02059538).
Study protocol	Study protocol is available from the study promoter: Assistance Publique-Hôpitaux de Paris (AP-HP).
Data collection	This is described in greater detail in the manuscript and companion manuscripts, and involve hospital regions of Paris, Copenhagen and Leipzig during period 2012-2016. The prospective cross-sectional multi-center study MetaCardis covered a wide range of metabolic and cardiac phenotypes. For the purpose of the study a total of 2,173 subjects including healthy controls as well as subjects with increasingly severe metabolic and cardiac disease were recruited into 8 study groups in Copenhagen, Denmark, at the university hospital of Leipzig, Germany and Assistance Public des Hopitaux (APHP), France. Subjects were free to answer their questionnaires at home and questionnaires were collected on the study day. Data pertaining to metabolic and metabolomics measurements stem from blood samples drawn on the study day after an overnight fast. Metagenomics data stem from sequencing of stool samples collected by the subjects no earlier or later than a week of their study visit.
Outcomes	Since the study was a cross-sectional non-intervention study, conventional outcomes were neither defined nor assessed. As such no primary or secondary outcomes were predefined or assessed. Assessed were metabolic health markers in association with microbiome and metabolome data. Disease status and patient groups were defined along international definitions of disease, with obesity defined according to the WHO criteria , metabolic syndrome according to the International Diabetes Federation, T2D by the American Diabetes Association and hypertension according to the American College of Cardiology and American Heart Association.

Flow Cytometry

Plots

Confirm that:

☒ The axis labels state the marker and fluorochrome used (e.g. CD4-FITC).

☒ The axis scales are clearly visible. Include numbers along axes only for bottom left plot of group (a 'group' is an analysis of identical markers).

☒ All plots are contour plots with outliers or pseudocolor plots.

☒ A numerical value for number of cells or percentage (with statistics) is provided.

Methodology

Sample preparation	0.2 g frozen (-80ºC) faecal aliquots were dissolved in physiological solution to a total volume of 100 mL (8.5 g/L NaCl). Subsequently, the slurry was diluted 1,000 times. Samples were filtered using a sterile syringe filter (pore size of 5 µm). 1 mL of the microbial cell suspension obtained was stained with 1 µL SYBR Green I (1:100 dilution in DMSO; shaded 15 min incubation at 37ºC).
Instrument	C6 Accuri flow cytometer (BD Biosciences, New Jersey, USA).
Software	BD Accuri CFlow software v1.0.264.21 (BD Biosciences, New Jersey, USA).
Cell population abundance	Not applicable. No sorting of fractions was performed.
Gating strategy	Fluorescence events were monitored using the FL1 533/30 nm and FL3 >670 nm optical detectors. In addition, also forward and sideward-scattered light was collected. The BD Accuri CFlow software was used to gate and separate the microbial fluorescence events on the FL1/FL3 density plot from background. A threshold value of 2000 was applied on the FL1 channel. The gated fluorescence events were evaluated on the forward/sideward density plot, as to exclude remaining background events. Instrument and gating settings were kept identical for all samples.

☒ Tick this box to confirm that a figure exemplifying the gating strategy is provided in the Supplementary Information.